TECTONICS, VOL. 14, NO. 5, PAGES, 1133-1152, OCTOBER 1995

Paleomagnetism, magnetic anisotropy, and mid-Cretaceous paleolatitude of the Duke Island (Alaska) ultramafic complex

Scott W. Bogue,[1] Sherman Gromme, and John W. Hillhouse
U.S. Geological Survey, Menlo Park, California

Abstract. We report paleomagnetic results from layered igneous rocks that imply substantial post mid-Cretaceous poleward motion of the Insular superterrane (western Canadian Cordillera and southeast Alaska) relative to North America. The samples studied are from the stratiform zoned ultramafic body at Duke Island, which intruded rocks of the Alexander terrane at the south end of the southeastern Alaska archipelago at about 110 Ma. Thermal and alternating field demagnetization experiments show that the characteristic remanence of the ultramafic rocks has high coercivity and a narrow unblocking temperature range just below the Curie temperature of magnetite. This remanence is likely carried by low-Ti titanomagnetite exsolved within clinopyroxene and perhaps other silicate hosts. The Duke Island intrusion exhibits a well-developed gravitational layering that was deformed during initial cooling (but below 540°C) into folds that plunge moderately to the west-southwest. The characteristic remanence clearly predates this early folding and is therefore primary; the Fisher parameter describing the concentration of the overall mean remanence direction improves from 3 to 32 when the site-mean directions are corrected by restoring the layering to estimated paleohorizontal. All samples exhibit a magnetic anisotropy that is strong but nonuniform in orientation across the intrusion, and we show that it has no significant or systematic effect on the site-mean directions of remanence. At least some of the anisotropy derives from secondary magnetite formed during partial serpentinization. The mean paleomagnetic inclination (56° ± 10°) corroborates paleomagnetic results from five coeval silicic plutons of the Canadian Coast Plutonic Complex to the south and southeast and implies 3000 km (± 1300 km) of poleward transport relative to the North American craton. Between mid-Cretaceous and middle Eocene time, the Insular superterrane and Coast Plutonic Complex shared a common paleolatitude history, with more poleward transport than coeval inboard terranes.

Introduction

The Canadian Cordillera, including southeastern Alaska, is divided into a series of physiographic/geologic provinces that are roughly parallel to the continental margin. From west to east, these are the Insular Belt, the Coast Plutonic Complex, the Intermontane Belt, the Omineca Crystalline Belt, and the Rocky Mountain Belt. Of these, both the Insular Belt (Terrane II) and the Intermontane Belt (Terrane I) are superterranes composed of smaller tectonostratigraphic terranes that are termed "suspect" because they are evidently allochthonous with respect to the North American craton [e.g., *Monger et al.*, 1982]. The Coast Plutonic Complex and the Omineca Crystalline Belt are the broad loci of sutures joining these two allochthonous superterranes to each other and to the continent. The Intermontane superterrane accreted to North America in Middle Jurassic time, and the outboard Insular superterrane accreted to the Intermontane superterrane sometime between the Middle Jurassic and Late Cretaceous [*Monger et al.*, 1982; *van der Heyden*, 1992; *Rubin et al.*, 1990]. A regionally extensive mid-Cretaceous thrust belt, evident in plutonic and metamorphic rocks of the Coast Plutonic Complex and adjacent terranes, may record the arrival of the Insular superterrane or the telescoping of the preexisting margin [*Rubin et al.*, 1990; *Gehrels et al.*, 1990; *Rusmore and Woodsworth*, 1991; *Haeussler*, 1992; *McClelland et al.*, 1992; *Rubin and Saleeby*, 1992]. All the associated kinematic indicators in the rocks marginal to the Insular superterrane show only orogen-normal contractional movement. The outlines of the individual terranes and the Coast Plutonic Complex are illustrated in Figure 1, which does not include the autochthonous Rocky Mountain Belt to the east.

Plate reconstructions show that the Kula plate moved rapidly northward with respect to North America during most of latest Cretaceous and earliest Tertiary time, so that the two plates experienced oblique right-lateral convergence. Estimates of the duration of this rapid relative motion range from approximately 25 million years [*Stock and Molnar*, 1988] up to 40 million years [*Engebretson et al.*, 1985]. Fault reconstructions [*Gabrielse*, 1985] and abundant paleomagnetic evidence from mid-Cretaceous and latest Cretaceous rocks [*Irving et al.*, 1985; *Marquis and Globerman*, 1988; *Irving et al.*, 1995a, b; *Wynne et al.*, 1995] both imply that the Intermontane superterrane, the Coast Plutonic Complex, and, by implication, the Insular superterrane all moved significantly poleward with respect to North America for distances up to 3000 km between 115 Ma and 50 Ma. (Because this reconstruction places much of British Columbia at the latitude of Baja in mid-Cretaceous time, it has become known as the "Baja BC" hypothesis [*Umhoefer*, 1987].) Some of the paleomagnetic results that indicate such great displacement are controversial. Several from the Coast Plutonic Complex are derived from plutonic rocks without layering or other features that can provide a straightforward measure of paleohorizontal. The possibility exists therefore that the inferred paleolatitudes are inaccurate because the plutons have been tilted since acquiring their remanence, and these arguments are carefully summarized by *Irving and Wynne* [1990, 1991].

[1]Now at Occidental College, Department of Geology, Los Angeles, California.

Paper number 95TC01579.
0278-7407/95/95TC-01579$10.00

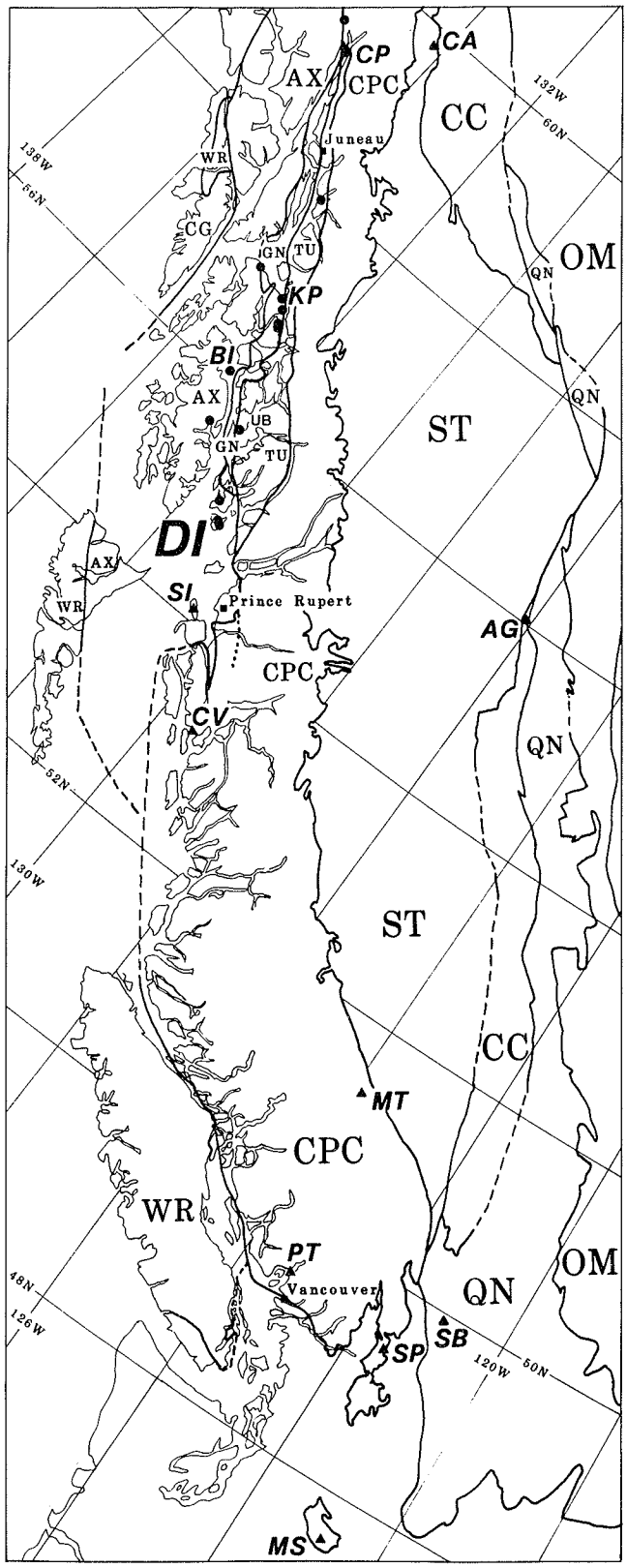

Figure 1. Simplified terrane map of the western Canadian and Alaskan Cordillera, after *Tipper et al.* [1981], *Silberling and Jones* [1984], and *Nokleberg et al.* [1994]. Geologic terranes are (from west to east) CG, Chugach; WR, Wrangellia; AX, Alexander; GN, Gravina Belt; TU, Taku; CPC, Coast Plutonic Complex (including Tracy Arm terrane); ST, Stikinia; CC, Cache Creek; QN, Quesnellia; OM, Omineca Crystalline Belt. Locations of southeastern Alaskan Cretaceous ultramafic complexes, some zoned, are taken from *Gehrels and Berg* [1984] and shown as circles: CP, Chilkat Peninsula; KP, Kane Peak; BI, Blashke Islands; UB, Union Bay; DI, Duke Island. All but Union Bay have associated paleomagnetic data. Other paleomagnetic localities are shown as triangles: in the Coast Plutonic Complex they are SI, Stephens Island pluton; CV, Captain Cove pluton; PT, Porteau pluton; SP, Spuzzum pluton (all described or cited by *Irving et al.* [1985, 1995a]); and MT, Mt. Tatlow [*Wynne et al.*, 1995]. In the Intermontane superterrane they are CA, Carmacks Group [*Marquis and Globerman,* 1988]; AG, Axelgold layered gabbro [*Monger and Irving,* 1980]; SB, Spences Bridge Group [*Irving et al.*, 1995b]. MS is the Mount Stuart batholith [*Beck and Noson*, 1972; *Beck et al.*, 1981; *Ague and Brandon*, 1992].

Lately, the discussions have focused on the mid-Cretaceous Mount Stuart batholith in the North Cascades of Washington at the southern end of the Coast Plutonic Complex. *Beck and Noson* [1972] and *Beck et al.* [1981] had obtained discordant paleomagnetic data from this pluton and posed the central question of whether the discordance resulted from translation or tilt. *Butler et al.* [1989] then showed that the structural attitudes in nearby younger sedimentary rocks could account for the paleomagnetic directions if the Mount Stuart batholith had originated only 500 km south of its present position and extended this argument by implication to the rest of the anomalous or discordant data from plutons of the Coast Plutonic Complex (see also *Umhoefer and Magloughlin* [1990], *Miller et al.* [1990], and *Butler et al.* [1990a, b]). Most recently, *Ague and Brandon* [1992] have used igneous (aluminum in hornblende) geobarometry to show that while the Mount Stuart batholith has indeed been tilted, after removal of this tilt the paleomagnetic inclinations still imply northward transport of almost 3000 km.

In this paper, we extend the mid-Cretaceous paleomagnetic record westward from the Coast Plutonic Complex into the Insular superterrane. We report remarkably self-consistent paleomagnetic and rock magnetic results derived from limited sampling (eight sites) of the 110 Ma ultramafic complex on Duke Island in southeast Alaska (Figure 1). Like coeval rocks of the western part of the Coast Plutonic Complex, the ultramafic complex of Duke Island intrudes late Paleozoic rocks of the Alexander terrane. Unlike the batholiths in the Coast Plutonic Complex, however, the Duke Island intrusion displays a cumulate layering so that inferred paleohorizontal can be estimated. Moreover, the layering has been broadly folded, and it is clear that the very stable remanence of the ultramafic rocks predates the folding. The only complication is that all units sampled at Duke Island are magnetically anisotropic. It is thus possible, in principle, that the paleomagnetism of the ultramafic complex of Duke Island does not accurately reflect the ancient field direction. We show, however, that the orientation of the anisotropy is not uniform throughout the intrusion, that the anisotropy does not have a systematic effect on the remanence directions, and that it is probably associated with a subpopulation of later-formed magnetic grains that does not carry the characteristic remanence.

The mean inclination from Duke Island, after correcting for folding, confirms the discordant mid-Cretaceous paleolatitudes derived from coeval batholithic and bedded rocks in the Coast Plutonic Complex by *Symons* [1977], *Beck et al.* [1981], *Irving et al.* [1985, 1995a], and *Wynne et al.* [1995].

Geologic Setting

The following summary of the geology of Duke Island is abstracted from the detailed descriptions by *Irvine* [1974] and *Saleeby* [1992]. The ultramafic complex on Duke Island (hereafter also referred to as the Duke Island ultramafic complex, for convenience) is one of several Alaska-type ultramafic igneous intrusive bodies [e.g., *Taylor*, 1967] that intrude the eastern edge of the Insular superterrane in southeast Alaska. It lies at the southern end of southeast Alaska (228.7°E, 54.9°N) and has an areal extent of approximately 155 km^2. Of this, about 23 km^2 is occupied by the ultramafic body itself. Ultramafic rocks crop out near Hall Cove, which cuts toward the island's center from the southwestern shore, and northwest of Judd Harbor on the island's southeastern side (Figure 2). Although aeromagnetic data [*Irvine*, 1974] suggest that these two outcrop units are surface expressions of a single igneous mass, it will be convenient to follow Irvine's informal unit terminology and refer to the two occurrences as the Hall Cove and Judd Harbor ultramafic complexes. The wall rocks comprise Ordovician to Silurian plutonic and metamorphic rocks and Late Triassic gabbro-diorite, all typical of the Alexander terrane exposed in this part of southeast Alaska [*Gehrels et al.*, 1987].

About 75% of the exposed ultramafic rock is olivine clinopyroxenite with varying but small amounts of hornblende. At Hall Cove, contact relations suggest that the innermost zone of olivine-rich rocks may represent a second, slightly younger intrusion. In all these rock types, serpentinization has affected some of the olivine but left the clinopyroxene intact except for some cracking due to alteration-induced expansion of neighboring olivine grains. The degree of serpentinization is less than 10%, except at some dunite localities. A hornblende-rich zone with outcrop widths of up to 600 m rims the ultramafic complex. Cumulate magnetite is present at some localities to the extent that the body is best described as hornblende-magnetite-clinopyroxene rock. The contact with the olivine clinopyroxenite is gradational over several meters and shows no evidence of being intrusive. The hornblende-rich nature of this zone probably reflects the interaction of the ultrabasic melt with water in the host rocks.

Although radiometric ages from the olivine-clinopyroxene

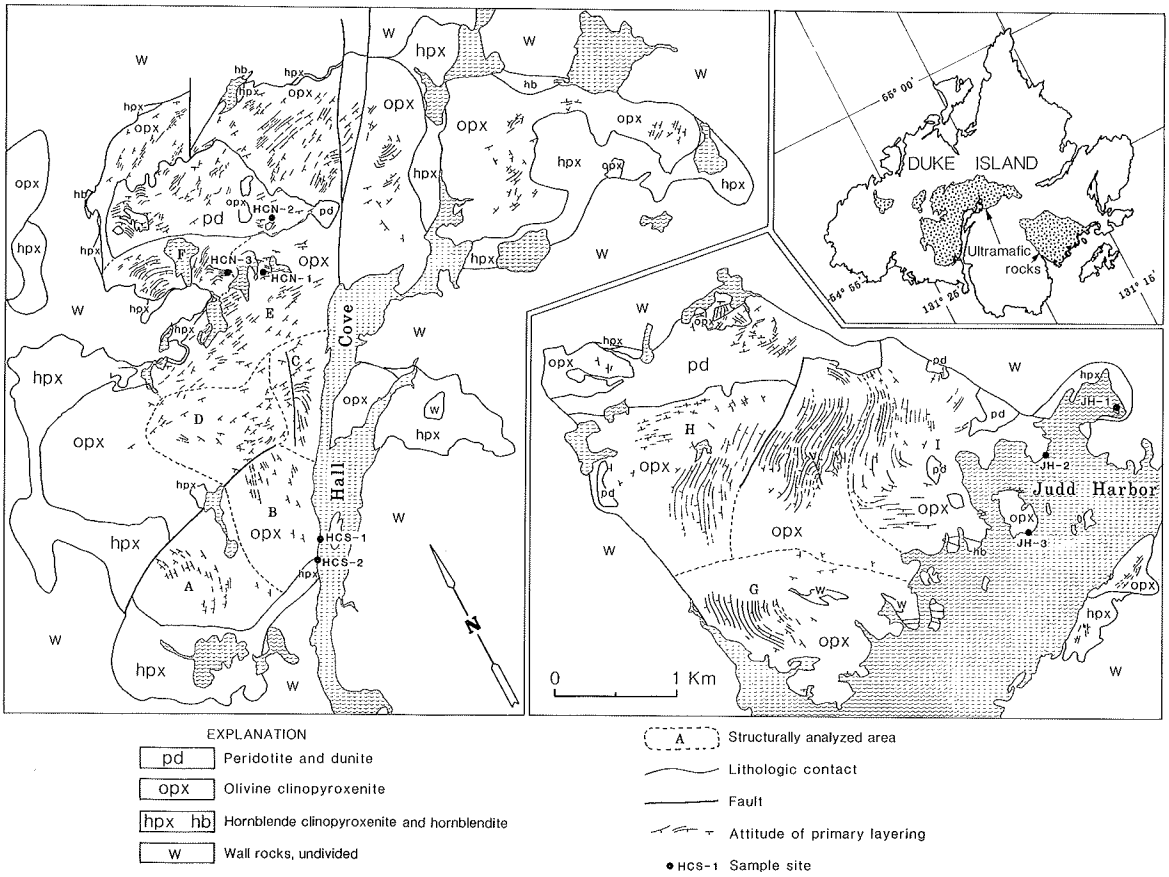

Figure 2. Partial geologic map of Duke Island, showing the two lobes of the ultramafic intrusion moved together for convenience (geological contacts and structural data from Plate 2 of *Irvine* [1974]). The areas that appear structurally homogeneous from Irvine's published map are delineated, and the paleomagnetic sampling sites are indicated. Attitudes of primary layering are indicated by tick marks pointing down dip of upright layering; numeric values of dips are omitted for clarity.

rocks are not available, both hornblende K-Ar [*Lanphere and Eberlein,* 1966; *Smith and Diggles,* 1981] and zircon U-Pb [*Saleeby,* 1992] dates have been obtained from hornblende-plagioclase pegmatites in the Judd Harbor body. Field and petrographic evidence [*Irvine,* 1974], as well as Sm-Nd studies [*Saleeby,* 1992], suggest that the pegmatites and olivine-clinopyroxene rocks are consanguineous, so that the ages from the pegmatites apply to the complex as a whole. These dates range from 106 Ma to 112 Ma and thus are in excellent agreement with K-Ar data from other Alaskan ultramafic bodies [*Lanphere and Eberlein,* 1966]. Additional ^{40}Ar-^{39}Ar ages of 115 Ma and 119 Ma have been reported by *Meen et al.* [1991]. Taken together, these ages represent an ultramafic intrusive episode along the length of the Insular terrane in southeast Alaska at about 110 Ma. Apparently, the intrusion of the Duke Island ultramafic complex just preceded the mid-Cretaceous orogeny affecting rocks of the Coast Plutonic Complex and eastern edge of the Insular superterrane.

Without a doubt, the outstanding feature of the Duke Island ultramafic complex is the spectacular cumulate layering present in the peridotite and olivine clinopyroxenite units, extensively illustrated by *Irvine* [1974]. Numerous sedimentary features, including graded bedding, angular unconformities, and local "soft-sediment" deformation features associated with slumped blocks (some with graded layering themselves), all attest to the cumulate nature of the ancient magma chamber. The laminations are defined by variations of grain size and composition; the local accumulation of settled grains creates millimeter to centimeter scale layers or zones in which the concentration of olivine relative to clinopyroxene can vary dramatically.

An episode of broad folding affected the ultramafic rocks; the evidence for this is illustrated in Figure 2. According to *Irvine* [1974], the rock was plastic (perhaps lubricated by small amounts of intercumulus liquid) when deformed, except in the highly strained hinge regions where some granulation is apparent. *Saleeby* [1992] reports undulose extinction and intergranular microbrecciation, especially in the Judd Harbor body, and interprets these features to represent "incipient" plastic deformation. In addition, *Saleeby* [1992] ties this episode of folding to the mid-Cretaceous orogeny mentioned above, thus supporting Irvine's conclusion that the folding occurred during original cooling of the pluton. As will be discussed in detail in the following section, fold axes in the Hall Cove and Judd Harbor bodies have similar orientations, trending in a SW-NE direction and plunging moderately to the southwest. A set of north-south, steeply dipping joints that clearly postdate the folding and are host to serpentine growth is also present in the Hall Cove body [*Irvine,* 1974; *Saleeby,* 1992]. Isotopic evidence cited by *Irvine* [1974] and his own observations strongly suggest that the serpentinization affecting olivines in the Hall Cove ultramafic complex resulted from hydration by meteoric water that was strongly localized by the jointing.

Remanence of the Ultramafic Complex

Paleomagnetic Methods

Core samples were obtained using a portable drill and oriented by magnetic compass. Backsighting to geographic reference points proved to be necessary because of the high latitude and magnetic nature of the rocks; compass deflections of over 90° were common in areas where lightning strikes were a problem, and weather precluded the use of a sun compass. Ten samples were collected from each of two sites (HCS-1 and HCS-2) near the south end of Hall Cove, from three sites northwest of Hall Cove (HCN-1, HCN-2, and HCN-3), and from three sites at Judd Harbor (JH-1, JH-2, and JH-3). Analysis of the remanence was performed with a three-component cryogenic magnetometer, tumbling alternating field (AF) demagnetization apparatus, and a shielded oven that allowed heating of samples in air in a field of less than 2 nT. Stepwise AF demagnetization experiments were performed on nearly all samples. The number of demagnetization steps varied from sample to sample depending on the results of detailed pilot work on several samples from each site, with 7 to 10 steps up to 0.1 T being typical. Two samples per site were

Table 1. Remanence Summary

	J_n		Rem/Ind		NRM Site-Mean Direction								Cleaned Site-Mean Direction						
Site (rock)	Med.	±%	Med.	±%	N	D	I	α_{95}	k	MMDF	MDT	Pk dJ/dT	N	D	I	D_s	I_s	α_{95}	k
HCS-1 (A)	10.5	26	7.16	32	10	059.1	61.0	6.9	49.9	42.5	-	-	10	062.2	62.0	327.1	69.3	6.9	50.3
HCS-2 (B)	20.9	77	2.56	74	10	062.6	46.5	32.2	3.2	36.7	549	560±22	10	054.5	48.7	355.8	61.6	10.5	22.2
HCN-1 (A)	10.3	31	37.70	87	10	353.0	21.9	3.0	265.3	>100	532	541±15	10	355.0	24.5	337.9	62.6	4.2	133.4
HCN-2 (C)	4.10	85	2.76	42	10	355.5	42.1	16.2	9.9	24.8	513	517±20	10	001.1	15.9	356.1	57.6	12.9	14.9
HCN-3 (D)	4.43	9	3.60	13	10	324.1	17.1	29.5	3.6	~50.0*	535	537±19	7	001.1	15.6	356.3	57.3	10.7	32.8
JH-1 (E)	36.3	61	3.06	56	10	107.5	49.3	7.9	38.8	23.0	538	542±17	9	117.9	37.8	343.6	41.4	5.6	84.9
JH-2 (A)	6.40	36	3.63	29	10	122.7	60.3	6.6	54.3	19.9	521	538±19	9	119.3	56.3	322.7	33.1	8.0	42.0
JH-3 (E)	25.5	49	23.34	14	10	130.1	23.7	4.1	137.9	17.6	554	560±22	10	130.5	24.1	357.2	56.4	6.7	52.8

J_n, natural remanent magnetization, A/m; ±%, percentage average variation; Rem/Ind, median ratio of remanent to induced magnetizations at site; Med.; median sample value; N, number of specimens averaged; D, declination eastward; I, inclination downward; α_{95}, radius of cone of 95% confidence centered on mean; k, Fisher precision parameter; MMDF, median value of median destructive fields in mT for AF demagnetization of J_n; MDT, median destructive temperature in degrees celsius for thermal demagnetization of J_n; Pk dJ/dT, temperature (°C) of maximum rate of decrease of J_n during thermal demagnetization; D_s and I_s, declination and inclination after compound structural correction (see text); A, massive olivine clinopyroxenite; B, hornblende-magnetite-clinopyroxene rock; C, layered peridotite; D, layered olivine clinopyroxenite; E, massive hornblende clinopyroxenite.

*Approximate value for five specimens not struck by lightning.

also subjected to detailed stepwise thermal demagnetization. We selected components of the remanence for further analysis by inspecting orthogonal vector diagrams for straight-line segments. The component considered to be the characteristic remanence for each specimen was that which trended toward or very nearly toward the origin. In virtually all cases, the characteristic remanence directions obtained by the thermal experiments were very similar to those derived from the AF demagnetizations.

Remanence Results

Table 1 summarizes the remanence properties and characteristic directions from the ultramafic sites on Duke Island. Many of the magnetic properties, such as the natural remanent magnetization (NRM) intensity or the median destructive field (MDF), vary considerably from sample to sample in a given site. Much of this variation is caused by a few samples with radically high or low values as compared with the remaining samples. We therefore give median values and the average variation from the median as a way of concisely reporting a property for the site without unduly emphasizing the extreme values. It is apparent even in the NRM directions that there is a consistency of directions within the groups of sites at north Hall Cove, south Hall Cove, and Judd Harbor and sizable angular differences between these three groups. All the directions are distinct from the present field (D = 27°, I = 74°) or a typical normal-polarity Tertiary field (D = 0°, I = 71°). The within-site angular dispersion is reasonably low except at HCS-2, HCN-2, and HCN-3.

We show the response of typical samples to AF demagnetization in Figure 3. A distinctive feature of these rocks is their relatively high bulk coercivity as suggested by the median value of specimen MDFs from each site (Table 1 and Figure 3). These values range from around 0.02 to greater than 0.1 T; many would be much higher were it not for the invariable presence of a recently acquired viscous remanent magnetization (VRM) with low coercivity. Figure 3 shows that after removal of the relatively soft VRM, the remaining remanence is typically very resistant to AF demagnetization. This property of the ultramafic rocks is particularly interesting with regard to the thermal demagnetization results that we discuss next.

Figure 4 shows the key features of the thermal demagnetization experiments. These features are summarized in Table 1 for all sites except HCS-1 (which was excluded because of excessive sulfide content). We report the details of just one of two samples studied from each site; demagnetization behavior was quite consistent between the replicates so that the values in Table 1 may be considered typical. For most samples, very little change in direction or intensity occurred during the first 500°C of heating, except that associated with the removal of minor VRM. With further heating, however, the drop in intensity was precipitous (see Figure 4). The "peak dJ/dT" listed in Table 1 is the tempera-

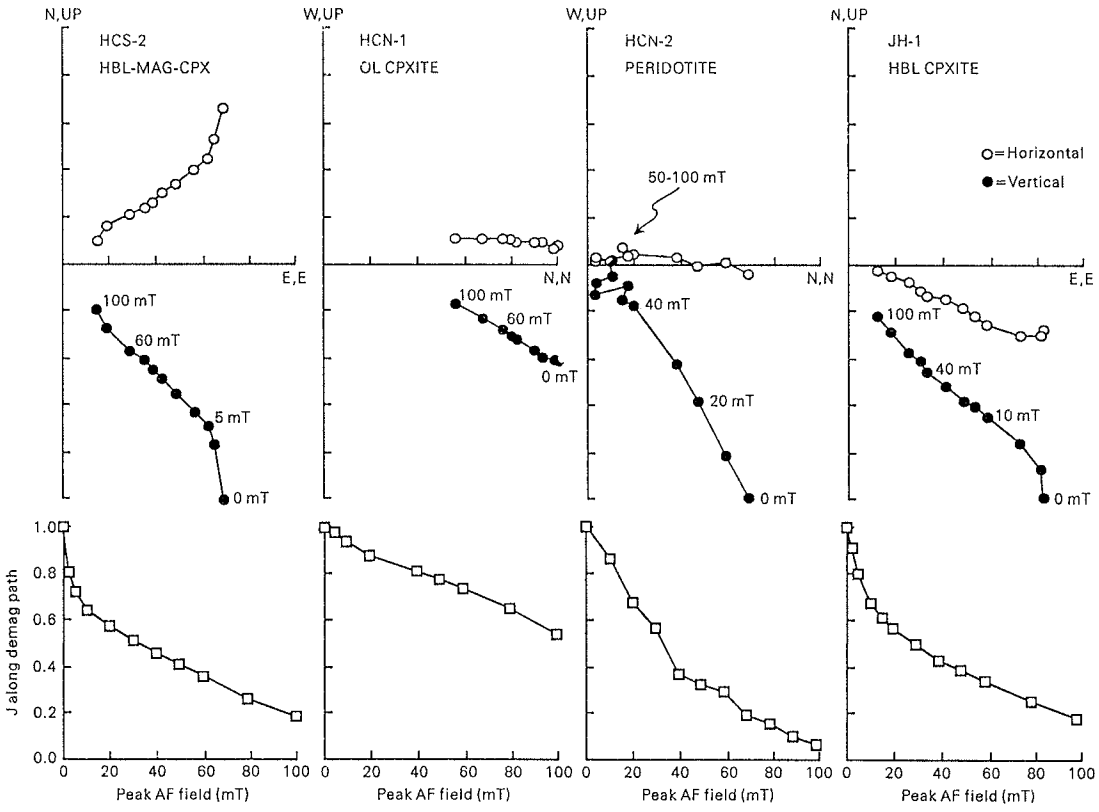

Figure 3. Response to alternating field (AF) demagnetization of four rock types (hornblende-magnetite-clinopyroxenite, olivine clinopyroxenite, peridotite, and hornblende clinopyroxenite) from the Duke Island ultramafic complex. Upper half shows orthogonal vector diagram. Lower half shows vector demagnetization path length versus AF field strength. Being independent of direction changes, this construction gives a clearer picture of the stability range of remanence components than plots of intensity versus field strength.

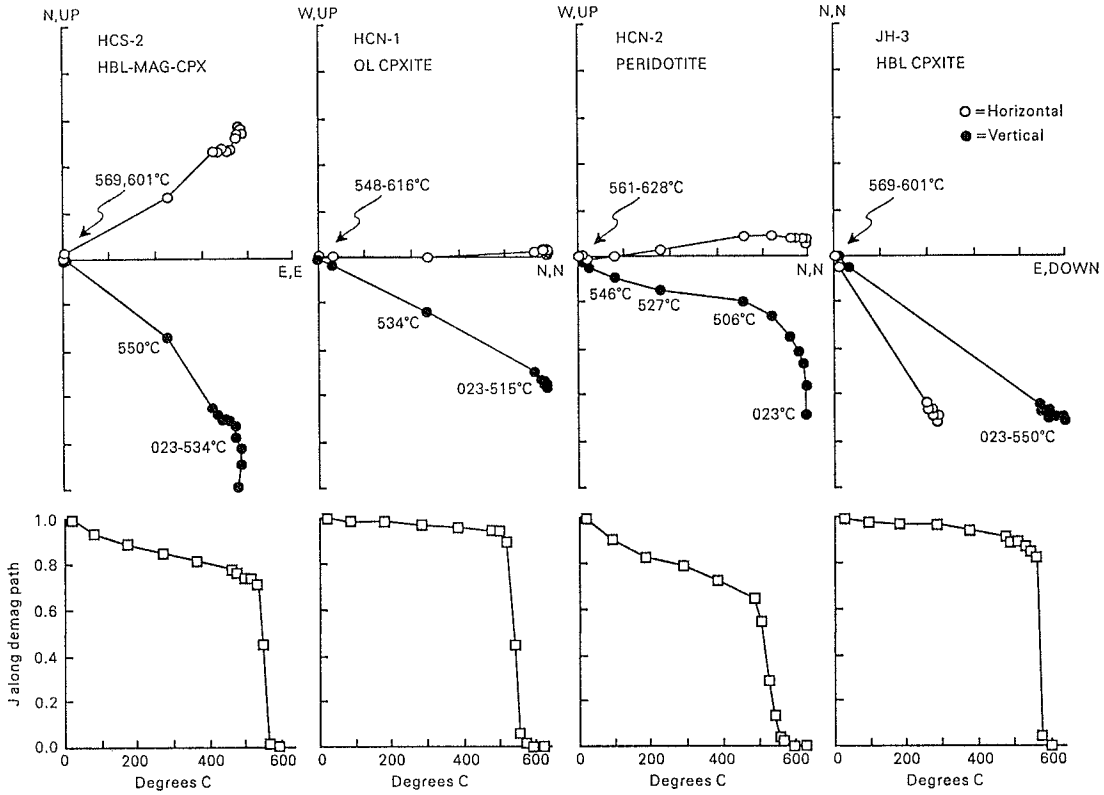

Figure 4. Response of typical samples to thermal demagnetization (see Figure 3 for explanation).

ture at which the magnitude of the vector component removed per °C of heating was greatest. This value corresponds to the temperature at the midpoint of the steepest segment on the curves at the bottom of Figure 4. Peak dJ/dT values, which range from 517°C to 560°C for these samples, correspond to peaks in the unblocking temperature (T_{ub}) spectra. The median destructive temperatures, which are also listed in Table 1, are always close to the peak dJ/dTs and attest to the very narrow T_{ub} ranges that characterize these samples. Any remanences remaining after heatings to temperatures higher than 580°C were small and not distinguishable from components that the samples began to acquire either from the small residual field (less than 2 nT) in the furnace or viscously during measurement. When plotted on orthogonal vector diagrams, the demagnetization trajectories trended directly to the origin after removal of any low T_{ub} components that were present.

A single component typically dominates the magnetization of the samples from each of the Duke Island sites. This component is isolated equally well by AF or thermal demagnetization techniques. The characteristic features of this remanence are its high coercivity and limited range of T_{ub}s near 540°C. The complete disappearance of the component by 580°C strongly suggests magnetite as the carrier; the high coercivities and unblocking temperatures suggest small grains with high intrinsic anisotropy, that we will argue below to be of magnetostatic (shape) origin.

The directions of the characteristic magnetization, summarized on the right side of Table 1 and plotted in Figure 5, are for the most part those obtained by analysis of the AF demagnetization experiments. The within-site dispersions of the characteristic magnetizations are less than those for the NRMs: for HCS-2, α_{95} for ten samples decreased from 32.2° to 10.5° although the mean direction changed by only 6°. Comparison to the NRM directions reveals that most cleaned site-mean directions are not much different from the respective NRM directions. The biggest changes, 35° for HCN-3 and 27° for HCN-2, greatly improved the grouping of site means from northwest of northern Hall Cove and emphasized the difference in direction between this group of sites and those from southern Hall Cove.

Structural Analysis and the Paleomagnetic Fold Test

The site-mean directions plotted in Figure 5 are distributed along a small circle, as would be expected if a once-uniform magnetization had been dispersed by folding. Indeed, as shown in Figure 5, the best fit small circle represents a cone that does not lie far from any of the data and whose axis trends 247° and plunges 12° SW. It is not straightforward, however, to restore the paleomagnetic directions to their original orientations. The abundance of crosscutting beds, soft-sediment deformation features, and other evidence of nonuniform topography at the bottom of the magma chamber means that local attitudes of crystal cumulate layering cannot be trusted to faithfully reflect paleohorizontal. Moreover, the folding that affected the layered rock on Duke Island occurred about axes that are now inclined from the horizontal (see structural closure patterns on Figure 2).

To properly correct the paleomagnetic data, we first inspected *Irvine*'s [1974] map and divided parts of the two ultramafic outcrop areas into seven domains that appeared to be structurally

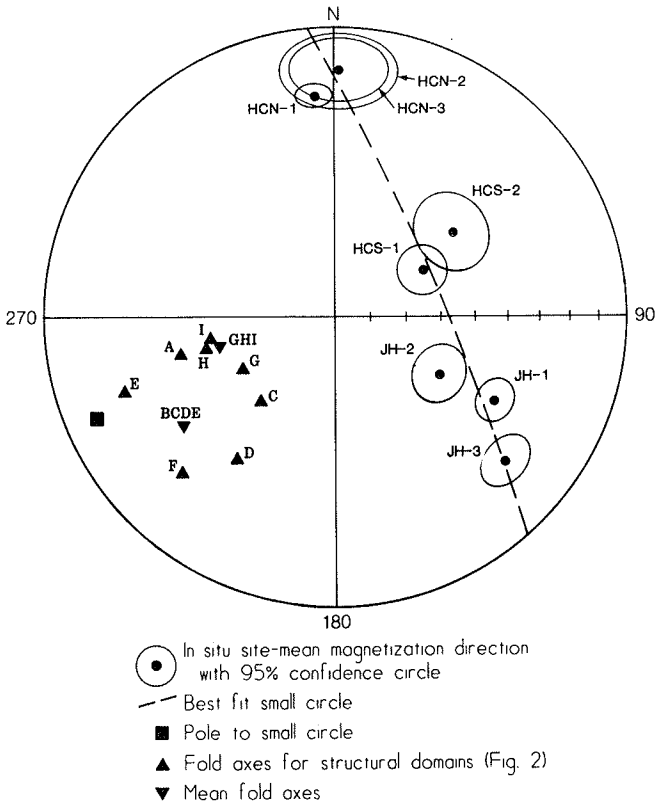

Figure 5. Equal-area projection on lower hemisphere of site-mean remanence directions in geographic coordinates, after magnetic cleaning. Letters shown by individual fold axes correspond to the contiguous areas shown in Figure 2. Mean fold axes are labeled BCDE for the Hall Cove body and GHI for the Judd Harbor body. The dashed line is the small circle (cone) best fit by least squares to the site-mean vectors; notice that its pole lies not far from the fold axes. Data are from Tables 1 and 2.

Table 2. Average Fold Axes and Attitude of Primary Layering

			Fold Axes		Average Layering	
Area	Site	N	Trend	Plunge	Strike	Dip
A		22	256	45		
C		19	221	58		
D		33	214	40		
E		37	250	24		
F		15	224	26		
B,C,D,E		100	234	36		
B	HCS	13			190	35
*	HCN	16			107	45
G		17	240	60		
H		23	256	53		
I		20	260	54		
G,H,I		60	256	56		
*	JH	8			253	80

Area, structurally analyzed areas outlined on Figure 2; Site, group of paleomagnetic sampling sites sharing a common structural correction; N, number of attitudes of primary layering scaled from Plate 2 of *Irvine* [1974]. Trend and strike, degrees east; Plunge and dip, degrees downward (sense of strike 90 deg counterclockwise from direction of dip).

* Homogeneous areas for these structural corrections are small and not shown on Figure 2.

homogeneous; that is, for which the assumption of cylindroidal folding looked reasonable (see Figure 2). Table 2 lists the poles to the great circles that best fit (in a least squares sense) the observed poles to primary (i.e., igneous) layering for each of the domains. These estimates of the fold axes are quite consistent in orientation (see Figure 5); the azimuths range from 214° to 260° and the plunges from 24° to 60°. *Irvine* [1974] estimated that the fold axis in the Hall Cove body trended 245° and plunged 50°W. It is apparent from this exercise that the folding of the ultramafic rocks on Duke Island is remarkably uniform in orientation across the island, much more uniform than one would gather from cursory inspection of the geologic map. One discernible trend is that the fold axes for the Judd Harbor body are somewhat steeper and more westerly than those for the Hall Cove body. The overall mean fold axes for the two bodies (see Table 2) differ by 25°, and so we have used these two axes rather than a grand mean axis for correcting the paleomagnetic data.

Also listed in Table 2 are mean primary layering attitudes calculated using *Irvine*'s [1974] map for small regions centered on the paleomagnetic sampling localities at northern Hall Cove, southern Hall Cove, and Judd Harbor. The Hall Cove localities are on opposite limbs and far from the hinge of a plunging syncline, and it was a straightforward matter to select the appropriate subsets of the structural data for the fold test. Although the structure of the Judd Harbor body is also well defined, the paleomagnetic sampling area is located far from places where the layering is well expressed. As a result, there is more uncertainty associated with the structural corrections applied to the paleomagnetic data from Judd Harbor.

We corrected the remanence directions by first rotating the mean layering attitudes about a horizontal axis perpendicular to the plunging fold axis by an amount that brought the fold axis

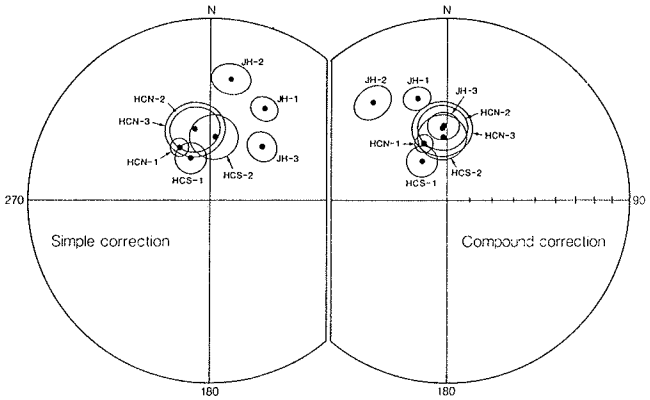

Figure 6. Equal-area projections on lower hemisphere of site-mean remanence directions after structural correction (Table 1), with circles of 95% confidence. (left) Data after simple tilt correction, rotation around mean strike line for groups of sites; (right) Data after compound correction, first removing plunge of fold axes (Table 2), then rotating around resulting new strikes of layering.

back to horizontal and then rotating the beds to horizontal about their (new) strikes. The corrected data are listed on the right side of Table 1 and plotted on Figure 6. The data group well after making this compound correction; the concentration parameter k for the site-mean remanence directions increases from 3.0 to 31.9. Restoring the mean layering attitudes to horizontal by simple rotation about the strike also increases k but only from 3.0 to 19.3. The contrasting results of these two correction schemes are illustrated in Figure 6. Using the significance test of *McFadden and Jones* [1981], the fold test is conclusive and positive (at 95% confidence) using the compound correction and inconclusive using the simple correction. The improved clustering of the directions after the two-stage correction shows clearly that the remanence is prefolding.

The success of the fold test also gives us confidence that the mean layering provides a reasonable estimate of paleohorizontal. Aeromagnetic data described by *Irvine* [1974] suggest that the Hall Cove and Judd Harbor ultramafic bodies are simply surface exposures of a single 15-km long intrusive complex that extends from just WNW of the Hall Cove body to East Island, about 5 km ESE of the Judd Harbor body. If the original cumulate layering departed substantially from paleohorizontal anywhere, it would most likely be near the walls of this ancient magma chamber. As can be seen in Figure 2, the Hall Cove and Judd Harbor localities are at opposite ends of the inferred extent of the pluton. At the northwest end, the southern Hall Cove sites lie close to a SW facing side of the intrusion, while the northern Hall Cove sites are closest to a north facing side. At the SE end, the Judd Harbor sites are close to a NE facing side. Substantial initial dips are clearly possible at all the paleomagnetic sites, but their orientation should vary greatly between the three localities. The positive fold test therefore provides strong evidence that the presence of variable initial dips has not seriously spoiled our estimates of paleohorizontal. We conclude that the paleomagnetic directions are properly restored and can be used to estimate paleolatitude.

Both *Irvine* [1974] and *Saleeby* [1992] discuss textural evidence suggesting that the folding occurred during original cooling while grains were at high enough temperatures to deform plastically. The paleomagnetic and rock-magnetic evidence, to be described more fully below, provides a more specific constraint: it requires nearly all the folding to have occurred after temperatures were below 540°C. This upper limit is not consistent with the inference of *Irvine* [1974] that the peridotite units (which show less textural evidence of penetrative strain) contained substantial intercumulus liquid during folding. Notice also that this evidence does not support *Irvine*'s [1974] conjecture that the deformation of the pyroxene- and hornblende-rich rocks resulted from the forcible emplacement of the peridotite body northwest of Hall Cove, a conjecture that *Saleeby* [1992] also could not corroborate. The tight grouping of the unfolded remanence directions, including those from HCN-2 which is situated within the peridotite, clearly implies that the peridotite is not much older than the surrounding rocks and that the ultramafic complex as a whole was deformed after cooling to at least 540°C.

After unfolding, the average remanence direction from eight sites is D = 343.9°, I = 55.7°, with an α_{95} of 10.0°. Using the current latitude and longitude of Duke Island and the North American reference pole (71.2°N, 194.1°E, α_{95}=3.7°) of *van Fossen and Kent* [1992], we calculate an expected Cretaceous field direction of D = 330.8°±7.7°, I = 78.6°±1.6°. The mean direction for the eight Duke Island sites lies 23.3° from the expected direction, and so the two are quite distinguishable, especially in inclination.

Magnetic Mineralogy

The opaque mineralogy of the ultramafic rocks from Duke Island was described in some detail by *Irvine* [1974]. We have supplemented this information with observations on one polished thin section made from one paleomagnetic specimen from each site.

There are at least three distinct populations of magnetic grains that are readily apparent in these rocks. The first includes relatively large grains of magmatic magnetite and pyrrhotite that are especially abundant in samples from southern Hall Cove and Judd Harbor. The magnetite at HCS-2 occurs as large (several mm) intergrowths with ilmenite and hercynite spinel. These grains are interstitial and have irregular, cuspoid shapes. Large magnetite grains are also seen at HCS-1 and JH-1. The pyrrhotite is typically intergrown with chalcopyrite and rare pentlandite. These magmatic phases, at least the grains that are visually striking, are probably not the source of the characteristic remanence; the high coercivities and narrowly distributed unblocking temperature ranges evident in the demagnetization experiments rule out the large magnetite grains, and the high unblocking temperatures evident in the thermal experiments rule out the pyrrhotite (which has a Curie temperature (T_c) of 320°C).

The second population consists of small, bladelike inclusions in silicate hosts (Figure 7). These grains are especially prominent in large oikocrysts of clinopyroxene (enclosing grains of olivine) at HCN-2 but are visible in samples from all sites except JH-1. In clinopyroxene grains, the inclusions typically have length-to-width ratios of 10 to 1 and are much thinner in the third dimension. Lengths range from a few to 75 microns. Although the largest grains are easily seen under the microscope, making identification possible, the smaller sizes are by far the most common. The thinnest of the lamellae are translucent with a dark grey-brown color that rules out hematite. The thickest lamellae display moderate reflectivity and gray color under reflected light. Electron microprobe analysis of 13 large lamellae from four sites demonstrates that the mineral is essentially magnetite (83.5 mole percent iron oxide calculated as Fe_3O_4) with approximately 3.3% TiO_2. Smaller amounts (less than 2.0% each) of MgO, Al_2O_3, and SiO_2 are present, and the approximately 8% that remains unanalyzed can probably be accounted for by small amounts of Cr, Mn, or similar metals.

Studies on a variety of igneous rock types (e.g., ocean-floor gabbro [*Davis,* 1981], gabbro [*Evans et al.,* 1968], diabase [*Hargraves and Young,* 1969], and anorthosite [*Murthy et al.,* 1971]) have shown that small inclusions of magnetite in either pyroxene or plagioclase can provide a very stable remanence. A similar explanation for the high-coercivity, prefolding remanence in the Duke Island rocks seems likely. Magnetite inclusions are common in clinopyroxene, the predominant mineral at five of the eight sampling sites. At sites HCS-2 and JH-3, hornblende is more common than clinopyroxene. Even though we cannot positively identify as a magnetic oxide the similar but much smaller lamellae that we observed in hornblende, the remanence properties (which are very similar to those for clinopyroxene-rich rocks) support our supposition that this mineral is also magnetite

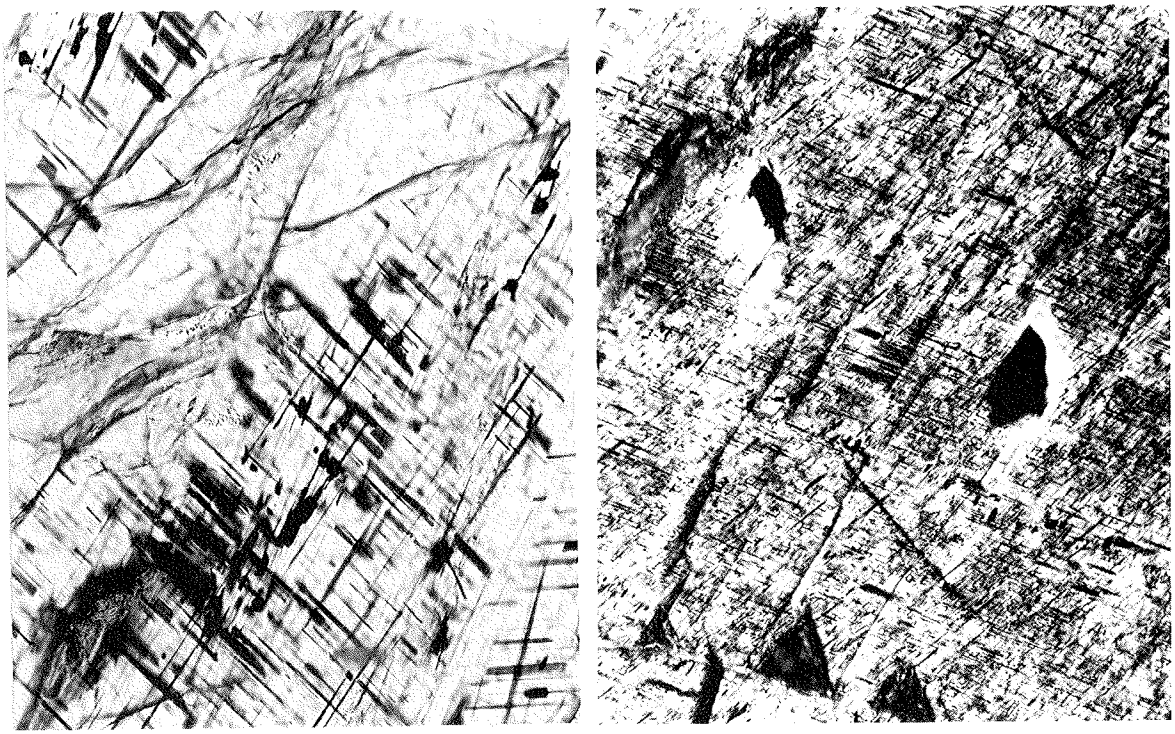

Figure 7. Photomicrographs of opaque inclusions in a clinopyroxene grain from site HCN-3 and a hornblende grain from site JH-3. The inclusions in the clinopyroxene grain are essentially magnetite and are inferred to be the carrier of the prefolding remanence in the clinopyroxene-rich samples. The inclusions in the hornblende are too small to analyze but are suspected to be magnetite based on the character of the prefolding remanence in the hornblende-rich samples.

and that these inclusions are likewise the source of the remanence. As noted by others cited above who have studied magnetite-bearing silicates, the large shape anisotropy of small platelike or rodlike grains explains why the observed coercivities are so much higher than usual for magnetite. In the Duke Island rocks, the presence of small amounts of Ti and perhaps other metallic ions has evidently reduced the T_c of the magnetite by 30°C to 40°C. The shape anisotropy of the grains has kept the unblocking temperature ranges very narrow and close to the inferred T_cs. In the appendix, we use the method of *Fleet et al.* [1980] to infer that the oxide lamellae exsolved from their host clinopyroxene grains at a temperature of 540° ± 25°. If we assume that the natural unblocking temperatures of the oxide lamellae were the same as the laboratory unblocking temperatures, and if our estimate of their exsolution temperature is correct, then the remanence they carry might properly be considered as transitional between a thermoremanent magnetization (TRM) and a high-temperature chemical remanent magnetization, since these grains would have been forming approximately at their T_c.

The third population of magnetic grains is associated with alteration of silicate grains, especially serpentinization of olivine. This form of magnetite is most significant in the olivine-rich sites, namely HCS-1, JH-2, and those from northern Hall Cove. In thin section, the serpentine typically occurs in bands that cut across grains of olivine. The most heavily altered olivine is roughly 35% serpentine (JH-2), but the degree of alteration is less at the other sites. The magnetite forms dusty inclusions throughout the serpentine and is often concentrated in a thin, medial strip that is typically thick enough to be visible under reflected light. According to *Irvine* [1974] and *Saleeby* [1992], the serpentinization in northern Hall Cove is controlled by a series of N to NNE trending joints. These joints, which are roughly parallel to the fault running down the length of Hall Cove, cut across the folds described above. Thus, for the Hall Cove sites at least, the magnetite associated with the serpentine is not carrying the primary, prefolding remanence.

Magnetic Anisotropy

Background

In general, a paleomagnetic remanence will be parallel to the ancient field direction only if the rock is magnetically isotropic. The presence of planar fabrics, such as the well-developed cumulate layering and the jointing near Hall Cove, led us to suspect that the ultramafic rocks on Duke Island might not meet this condition. If consistently and favorably oriented across the outcrop area, a strong magnetic anisotropy could bias the mean remanence direction and therefore the estimated paleolatitude. An

anisotropy with variable orientation could produce a more benign effect: an increase in the within-site or between-site dispersion of remanence directions [e.g., *Hargraves,* 1959].

We examined two kinds of magnetic anisotropy in the Duke Island samples: the anisotropy of (weak-field or initial) magnetic susceptibility (AMS), and the anisotropy of isothermal remanent magnetization (AIRM). The experimental methods are described in the appendix. The AMS, determined for an inducing field strength of 50 μT, is sensitive to the anisotropy intrinsic to the fraction of magnetic grains with lowest coercivity. We determined the AIRM for two higher coercivity fractions: from 10 mT to 20 mT (which we term the AIRM-lo) and from 30 mT to 40 mT (which we term AIRM-hi). The AIRM is particularly interesting because, in many rocks, it is identical in orientation and magnitude to the anisotropy of TRM (ATRM) [*Stephenson et al.,* 1986], the anisotropy most relevant to the primary remanence in an igneous rock. The practical advantage of using AIRM as a measure of the ATRM is that one avoids possible complications of chemical alteration caused by heating in the laboratory.

Character and Origin of the Anisotropy

Table 3 summarizes the magnetic anisotropy of samples from the Duke Island ultramafic complex. The values listed are derived from the site-mean susceptibility tensor computed as described in the appendix. Table 4 and Figure 8 show error limits for the AMS results estimated using a bootstrap technique similar to that of *Constable and Tauxe* [1990]; details can be found in the appendix. The sample data per site were too few to calculate meaningful errors for the AIRM determinations.

It is clear from Table 3 that the ultramafic rocks on Duke Island are very anisotropic and that the magnitude of AIRM-hi is roughly twice that of AMS. The average ratio of the maximum susceptibility (K_{max}) to the minimum susceptibility (K_{min}) for AMS is 1.18; that is, the difference between K_{max} and K_{min} is 18%. If expressed as the difference between K_{max} and the average of K_{max}, K_{int} (the intermediate susceptibility), and K_{min}, then the anisotropy is 16%. For the AIRM-lo and AIRM-hi, the anisotropies are 33% and 41% (K_{max} versus K_{min}) or 28% and 32% (K_{max} versus average K). As discussed by *Stephenson et al.* [1986], anisotropy of remanence is greater than AMS in most rocks. Figure 9 shows the normalized principal susceptibilities from the site-mean AMS and AIRM plotted against one another. Lines fit to the data resemble those shown in Figure 9 of *Stephenson et al.* [1986] for a variety of rock types. It is very clear that the anisotropy of the ultramafic rocks from Duke Island does not arise solely from a preferred alignment of uniaxial single domain grains; if it did, the plots in Figure 9 would have negative slopes and x intercepts near 0.5 [*Stephenson et al.,* 1986].

Table 3. Anisotropy Summary

				Geographic				Stratigraphic			
				K_{max}		K_{min}		K_{max}		K_{min}	
Site	N	Max %	Int %	D	I	D	I	D	I	D	I
Site-Mean AMS											
HCS-1	9	16.7	6.7	194.2	61.0	94.2	5.5	229.8	44.3	84.4	40.3
HCS-2	8	14.4	12.3	341.1	72.9	126.9	14.3	293.3	44.5	129.8	44.4
HCN-1	8	25.1	19.1	278.6	40.2	121.8	47.5	260.2	22.5	159.8	23.8
HCN-2	8	11.4	8.3	27.1	3.9	288.4	65.5	40.5	47.5	238.7	41.0
HCN-3	7	28.4	22.6	201.2	10.8	75.1	72.1	30.4	33.6	180.0	52.3
JH-1	5	16.0	9.5	96.3	17.0	311.0	69.6	11.6	25.4	105.0	7.1
JH-2	9	14.7	9.1	243.9	8.0	339.0	31.9	212.0	10.1	110.9	47.6
JH-3	7	16.8	12.8	252.0	21.9	352.8	24.8	227.1	4.5	131.1	53.5
Site-Mean AIRM-lo (20 mT-10 mT)											
HCS-1	3	18.2	6.2	185.1	43.6	301.3	24.9	207.7	37.0	111.5	8.1
HCS-2	3	38.5	26.0	30.9	21.6	299.3	4.0	6.0	29.4	114.1	28.9
HCN-1	7	28.3	24.4	306.1	13.6	108.6	75.8	299.3	23.1	185.6	43.3
HCN-2	4	16.6	11.3	3.3	37.8	216.3	47.3	327.7	77.3	218.4	4.3
HCN-3	4	43.2	19.1	187.3	10.8	59.1	72.8	14.1	33.1	184.2	56.6
JH-1	2	51.6	29.6	122.3	33.4	281.9	54.9	347.4	46.4	85.2	7.4
JH-2	3	31.4	17.4	241.6	20.7	147.7	10.1	224.6	14.0	25.3	75.2
JH-3	2	34.8	24.2	253.1	7.3	345.5	18.2	212.9	1.0	121.1	61.3
Site-Mean AIRM-hi (40 mT-30 mT)											
HCS-1	2	34.1	16.3	163.5	44.1	342.1	45.9	194.1	49.0	314.3	23.6
HCS-2	1	44.8	33.1	62.4	28.4	327.9	8.2	31.0	52.1	141.7	15.4
HCN-1	2	26.6	10.7	292.1	32.3	175.1	35.7	274.5	25.8	7.7	6.5
HCN-2	1	28.5	20.7	43.8	40.7	262.8	42.0	111.4	69.9	250.0	15.4
HCN-3	2	22.5	14.8	54.3	2.4	144.3	0.3	73.9	35.9	324.1	25.0
JH-1	1	38.7	20.6	128.5	9.7	244.0	68.3	23.6	56.3	273.7	12.8
JH-2	2	37.8	12.6	243.1	12.1	351.9	56.3	216.0	11.5	121.1	22.9
JH-3	1	94.7	73.8	255.4	13.7	348.1	10.9	39.6	0.1	129.8	68.1

Max%, $100[(K_{max}/K_{min})-1]$; Int%, $100[(K_{int}/K_{min})-1]$. Other symbols as in Table 1.

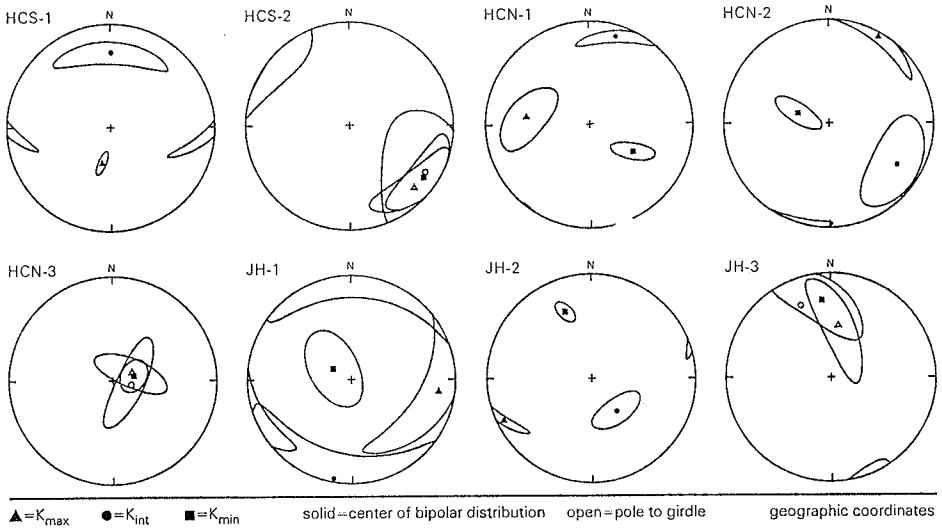

Figure 8. Lower hemisphere equal-area plots showing 95% confidence ellipses on site-mean AMS in geographic coordinates. Each ellipse corresponds to either the pole of a bipolar distribution or the pole to a girdle distribution, depending on which best describes the data. See appendix and Table 4 for more details.

Instead, the magnetic grains producing the anisotropy must include multidomain, pseudosingle domain, or perhaps interacting single-domain grains.

Although the AMS, AIRM-lo, and AIRM-hi are each characteristic of a particular coercivity fraction, there is considerable similarity between the fabrics (see Figure 10). For some sites (e.g., HCN-1, HCN-2, JH-1, and JH-3), the K_{max} and the K_{min} axes for all three anisotropies group well. At HCS-1 and JH-2, the K_{max} directions group better than the K_{min} directions, while at HCS-2 the opposite is true. For HCN-3, the pattern is more complicated; the K_{min} and K_{max} directions for the AMS are similar to those for the AIRM-lo but very different from those for the AIRM-hi. As shown in Figure 11, the plane containing the K_{max} and K-int directions (the magnetic foliation plane, which is perpendicular to the K_{min} direction) for the AMS and the AIRM-lo is oriented nearly parallel to the cumulate layering which here dips shallowly to the southwest. In contrast, the plane containing K_{max} and K-int for ARM-hi parallels the planar zones of serpentine and dusty magnetite that are visible in the paleomagnetic cores and thin sections. These mineralized planes are the sample scale manifestation of the jointing that cuts through folded layering at the Hall Cove localities. The K_{max} directions for all three anisotropies lie very close to the intersection of the cumulate layering and these magnetite-rich planes.

It is clear at HCN-3 that a component of the magnetic anisotropy arises from secondary magnetite associated with serpentine localized by joints. This phenomenon is similar to the one described by *MacDonald and Ellwood* [1988] in their study of a more highly serpentinized peridotite body in Venezuela. At HCN-3, however, the link between the K_{max} direction and the cumulate layering suggests that the anisotropy is composite, involving at least one other of the magnetic subpopulations present in the samples. The exsolved lamellae of magnetite are strongly oriented within their silicate hosts, but clinopyroxene grains at Duke Island show only a weak tendency to align in the cumulate layers [*Irvine*, 1974]. It does not seem likely therefore that the lamellae could produce a coherent, site-scale anisotropy. The large magmatic magnetite grains are not abundant at HCN-3 nor did we observe a preferred orientation of grain shapes at sites where this subpopulation was more prominent. Nevertheless, we cannot rule out the possibility that a subtle fabric may exist and only be apparent in samples much larger than the ones we examined (which were cut from standard paleomagnetic cores). If such a fabric did exist, it could help account for the low-coercivity component of the anisotropy at many sites (but not HCN-3). A complete discussion of the origin of the anisotropy is beyond the scope of this paper, but it seems likely that there is no simple explanation of the anisotropy that is applicable to the intrusion as a whole. None of the three magnetic subpopulations is abundant at all the paleomagnetic sites, and the orientation of the anisotropy is variable and (at HCN-3 at least) related to both prefolding and postfolding structure. These observations accord well with our inability (discussed below) to detect any systematic bias or increased dispersion in the remanence that is traceable to the observed anisotropy.

Effect on Primary Remanence Direction

Can the strong magnetic anisotropy of these rocks explain the shallowness of the primary remanence direction? We were motivated to answer this question because of the tendency (noticeable in Figure 10) of the site-mean remanence to lie near the site-mean magnetic foliation planes. If the anisotropy has had a systematic effect, then it should display two characteristics: it would have to be a prefolding feature of the rocks, and it would have to be oriented properly with respect to the ancient field direction. The first characteristic can be checked by comparing the anisotropies before and after correction for the folding. The test is not as straightforward as it is with remanence directions, however, because the orientation of the prefolding anisotropy (if present) may not have been uniform. If the anisotropy were related to the attitude of local bedding, for example, which in many places showing festoon crossbedding may have had significant

Table 4. AMS Results in Geographic Coordinates

Site-Mean AMS					Bootstrap Confidence Ellipse								
Magnitude			Direction		Center			Semimajor Axis			Semiminor Axis		
AMS %	Lo	Up	D	I	BG	D	I	D	I	Ang	D	I	Ang
					Site HCS-1 N=9								
16.7	1.2	1.0	194.2	61.0	B	194.1	61.1	23.4	28.6	10.4	291.2	3.9	3.0
6.7	1.6	2.3	1.2	28.4	B	0.5	28.1	91.9	2.7	40.0	186.9	61.8	10.0
	2.9	2.1	94.2	5.5	B	93.8	5.9	0.3	30.3	39.9	193.7	59.0	3.9
					Site HCS-2 N=8								
14.4	0.7	2.9	341.1	72.9	G	134.0	14.9	226.1	8.0	31.6	343.4	73.1	14.0
12.3	2.4	1.2	219.3	9.2	G	122.1	16.9	336.6	69.8	47.8	215.4	10.8	32.4
	3.1	1.4	126.9	14.3	B	125.8	14.6	217.2	5.5	29.5	327.4	74.4	14.7
					Site HCN-1 N=8								
25.1	2.9	6.6	278.6	40.2	B	277.5	38.9	34.6	29.5	29.9	149.9	37.1	15.1
19.1	2.0	1.5	18.7	11.7	B	17.3	11.9	281.0	27.5	27.3	128.4	29.6	5.5
	5.1	2.8	121.8	47.5	B	122.3	48.8	277.6	38.5	18.9	17.7	12.4	6.2
					Site HCN-2 N=8								
11.4	1.5	1.7	27.1	3.9	B	30.0	5.1	121.6	17.6	33.1	284.3	71.6	6.5
8.3	2.3	2.4	118.8	24.1	B	122.3	24.8	28.5	8.2	33.5	281.4	63.7	22.2
	3.4	2.8	288.4	65.5	B	288.6	65.0	123.5	24.2	21.5	30.9	5.7	7.5
					Site HCN-3 N=7								
28.4	2.4	5.6	201.2	10.8	G	67.5	73.7	299.4	10.3	30.9	207.0	12.6	11.0
22.6	5.4	2.7	294.0	14.1	G	99.7	75.7	209.0	4.8	39.3	300.1	13.5	10.9
	5.3	4.6	75.1	72.1	B	77.2	72.6	207.0	11.4	13.5	299.7	13.1	9.9
					Site JH-1 N=5								
16.0	0.3	4.2	96.3	17.0	B	98.0	17.2	196.6	25.6	67.4	337.7	58.4	15.4
9.5	3.3	1.9	189.7	10.9	B	190.4	3.9	281.0	8.6	65.3	76.3	80.5	25.4
	3.9	1.6	311.0	69.6	B	301.6	73.3	155.3	14.0	33.0	63.0	8.9	19.0
					Site JH-2 N=9								
14.7	1.0	3.0	243.9	8.0	B	244.6	7.2	147.0	46.3	21.3	341.3	42.8	3.4
9.1	1.4	1.0	141.5	56.9	B	143.4	57.3	235.8	1.5	21.2	326.8	32.6	10.2
	1.2	0.9	339.0	31.9	B	338.9	32.0	128.7	54.2	10.8	239.6	14.5	4.8
					Site JH-3 N=7								
16.8	2.0	5.6	252.0	21.9	G	8.2	48.9	154.8	36.1	47.4	257.7	17.0	12.0
12.8	2.3	2.8	125.7	55.8	?	-	-	-	-	-	-	-	-
	7.5	3.2	352.8	24.8	B	354.1	26.3	115.7	46.7	41.7	246.4	31.6	16.6

For each site, the first row describes K_{max}, the second row decribes K_{int}, and the third row describes K_{min}. AMS %, percentage referred to K_{min} (see explanation for Table 3); Lo and Up, 5th and 95th percentile limits derived from bootstrap procedure; BG: bipolar (B) or girdle (G) distribution of axes (sample K_{int} data for JH-3 fit neither distribution); Ang, length in degrees of semiaxis; D and I, see Table 1 for explanation.

original dip, then its orientation might have varied significantly from one part of the intrusion to another.

We examined the directions of maximum and minimum susceptibility for all three anisotropies in both geographic and stratigraphic coordinates (using the same compound correction scheme as with the remanence directions). The K_{max} directions show no strong pattern in geographic coordinates. In stratigraphic coordinates, however, the K_{max} directions for each anisotropy lie near a steeply dipping plane that trends NE-SW (Figure 12, lower left) suggesting a fabric that is prefolding. The opposite pattern, however, is seen in the K_{min} directions; the most coherent pattern is seen when the axes are plotted in geographic coordinates, suggesting a postfolding fabric (Figure 12, upper right). The contradictory evidence from the K_{max} and K_{min} data means that the fold test on the age of the anisotropy is inconclusive, probably because the premise of uniform anisotropy in either coordinate system is false.

We therefore turn to a much more direct approach to the problem of whether the shallow remanence of the Duke Island ultramafic complex is an accurate measure of the ancient field direction. For each sample, we computed the ancient field direction consistent with the observed remanence direction and anisotropy. The calculation consists simply of multiplying the remanence vector for a sample times the inverse of the 3 x 3 matrix representing the anisotropy tensor of the sample. If the anisotropy of TRM acquisition is assumed to be similar to the AMS or AIRM, then the result of this calculation will be a better estimate of the ancient field direction than the remanence direction itself. As mentioned above, this assumption is probably much better for the AIRM than for the AMS, but we investigated both kinds

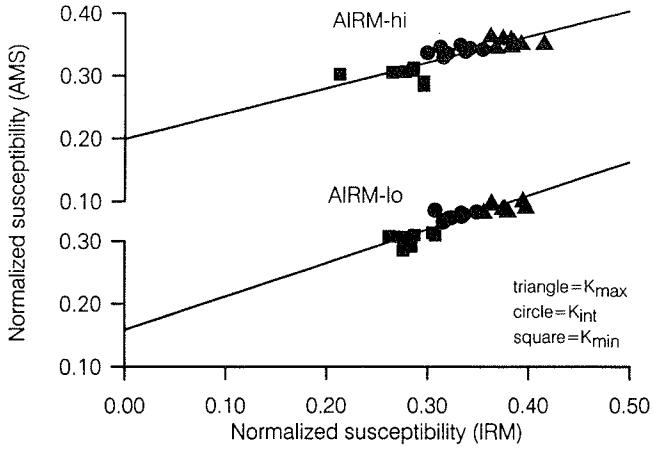

Figure 9. Plots of normalized susceptibilities (e.g., $K_{max}/(K_{max}+K_{int}+K_{min})$ of AMS versus AIRM-lo and AIRM-hi. As discussed by *Stephenson et al.* [1986], positive slopes and x intercepts well below 0.5 indicate that the anisotropy does not arise from noninteracting single-domain magnetite grains.

looking for any hint of systematic effects. Besides revealing any possible directional bias, this approach can show whether the anisotropy, which is somewhat variable in orientation from sample to sample, has dispersed the remanence directions around their site means (i.e., relative to the inferred field directions). The lack of such increased dispersion would be a clue that the anisotropy we are measuring has not significantly affected the ancient remanence and might thus be a younger feature of the rocks.

Table 5 presents a comparison of remanence untilted via the compound correction with inferred field directions. Of the eight site-mean inferred field directions calculated using the AMS data, four are steeper and four are shallower than the observed remanence directions. The overall mean inferred field direction (each sample given unit weight) is only 0.9° steeper than the mean remanence. For five of the sites, the inferred field directions group better than the remanence directions (i.e., their "dS" values in Table 5 are positive), although all the differences are small. If the remanence of the samples has been deflected by a fabric like that evident in the AMS results, then almost none of the anomalously shallow inclination or the observed within-site or between-site dispersion is due to anisotropy.

The calculated effect of the AIRM, though larger than that of the AMS, is still insignificant compared to the inclination anomaly to be explained. At HCN-3, which is characterized by very high anisotropy, the inferred field direction is 7.3° steeper than the observed remanence. If this site were typical, and if the primary remanence of the Duke Island ultramafic rocks were affected by a similar anisotropy, then about one-third of the inclination anomaly could be attributed to a rock magnetic effect. The remaining sites, however, yield inferred field directions that are closer to the remanence direction, with some deflected in the sense opposite that needed to explain the shallowness of the inclinations. The overall mean inferred field and remanence directions differ by only 2.8°. For the AIRM-hi, the mean directions differ by 1.5°, with the inferred field being shallower than the remanence. Evidently, the anisotropy we have detected in the samples, though perhaps capable of significantly affecting the remanence direction at some sites, is not uniform enough in magnitude or orientation to bias our estimate of the paleolatitude of Duke Island by more than a few degrees. It is also clear from Table 5 that little of the between-sample (within-site) directional dispersion is due to any anisotropy similar in orientation and magnitude to the AIRM. At five out of six sites for AIRM-lo, the inferred field directions are more scattered than the remanence directions (dS negative), at four sites substantially so. This observation is clearly inconsistent with the hypothesis that the primary remanence is systematically deflected by the anisotropy we have measured. We conclude therefore that the primary re-

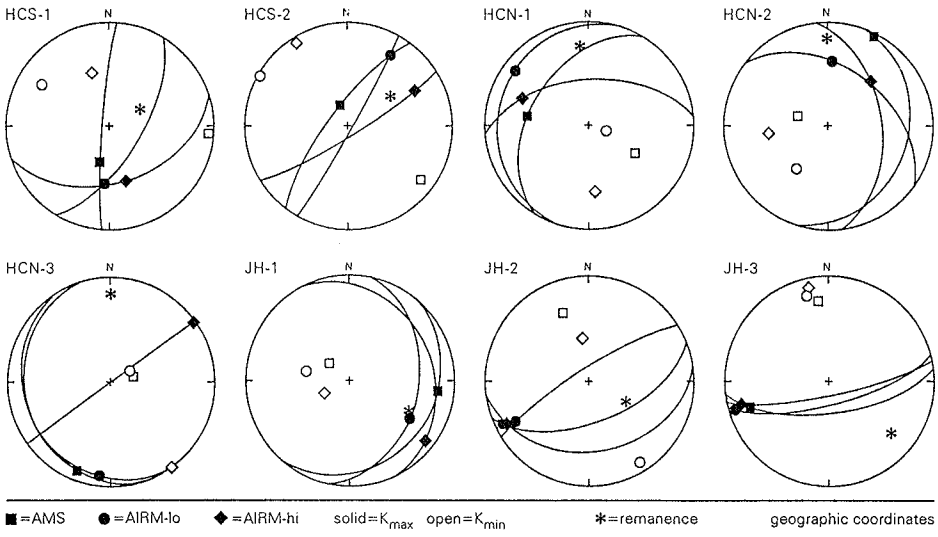

Figure 10. Lower hemisphere equal-area plots showing the orientations of site-mean AMS, AIRM-lo, and AIRM-hi in geographic coordinates (see Table 3). The great circles indicate the planes containing the directions of maximum and intermediate susceptibility; that is, the magnetic foliation planes. Also shown are the site-mean remanence directions, which by chance lie close the magnetic foliation planes at several sites.

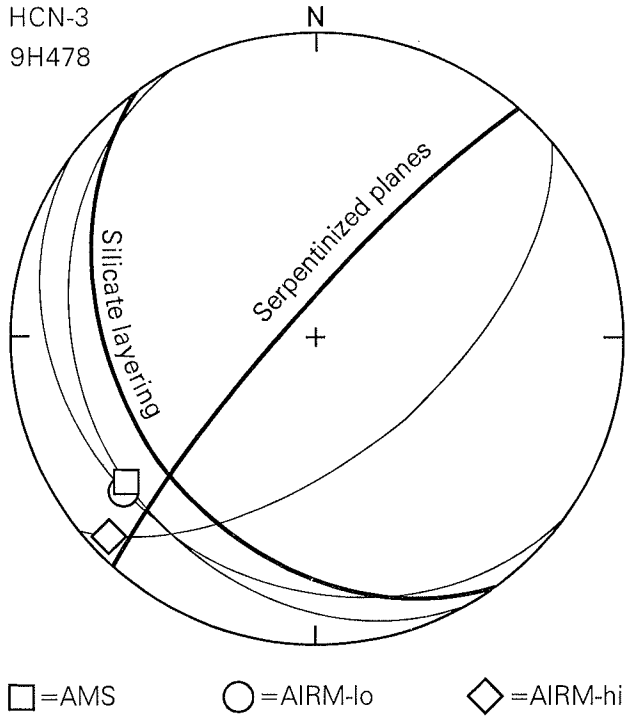

Figure 11. Lower hemisphere equal-area plot comparing anisotropies with other structural features for a sample from HCN-3 (geographic coordinates). The directions of maximum susceptibility for AMS, AIRM-lo, and AIRM-hi lie very close to the intersection of serpentinized planes rich in magnetite and the crystal layering (both shown as heavy great circles). The magnetic foliation planes (containing the directions of maximum and intermediate susceptibility and shown as light great circles) lie close to the crystal layering for AMS and AIRM-lo but closer to the serpentinized plane for AIRM-hi.

manence has accurately recorded the ancient field and that the tendency of the remanence direction to be near the magnetic foliation (see Figure 10) is fortuitous.

Other Cretaceous Ultramafic Rocks

Four other major areas of mid-Cretaceous ultramafic intrusive rocks, and a few minor ones, are approximately aligned along the Alaskan archipelago north of Duke Island. The major ones are the Chilkat Peninsula, Kane Peak and localities nearby to the south, the Blashke Islands, and Union Bay (Figure 1). All the ultramafic intrusions along this trend are the same age as the Duke Island ultramafic complex [*Lanphere and Eberlein,* 1966], and they intrude either Wrangellia, the Alexander terrane, or the Gravina Belt, but unlike Duke Island, none of them exhibits any primary gravitational layering or other evidence of paleohorizontal. Paleomagnetic data exist for three of these (Chilkat Peninsula, Kane Peak, and Blashke Islands) (S.W. Bogue and S. Gromme, unpublished data, 1985). Their remanence is very stable and of normal polarity, but the directions are steeper than the structurally corrected result from Duke Island. Lacking the constraints provided by paleohorizontal indicators, one can freely interpret these directions as ancient, indicating no significant tilting or latitudinal transport since the mid-Cretaceous, or as late Tertiary, products of partial or complete remagnetization. Both interpretations, however, are problematical. The first would imply that the Duke Island ultramafic body and the rocks it intrudes were tectonically disjoint from similar rocks of the same terranes to the north. To our knowledge, no geologic evidence exists for such a separation. Furthermore, this interpretation would be very difficult to reconcile with evidence [*Marquis and Globerman,* 1988] (site CG on Figure 1) that crust well inboard of the ultramafic sites has undergone significant latitudinal transport since latest Cretaceous time. The Tertiary remagnetization hypothesis implies a thermal history that is inconsistent with the concordant K-Ar ages from biotite and hornblende reported by *Lanphere and Eberlein* [1966]. A more complete discussion of these problems will occur elsewhere, but it may be that the paleomagnetic directions from these other ultramafic bodies have only local structural significance.

Tectonic Implications

Irving et al. [1985] had originally shown that five intrusive bodies from the Coast Plutonic Complex with radiometric ages ranging from 80 Ma to 115 Ma have magnetizations that are consistently shallow and easterly with respect to expected directions derived from the North American apparent polar wander path. The locations of these intrusive bodies are shown on Figure 1; they are the Captain Cove and Stephens Island plutons [*Symons,* 1977], the Spuzzum and Porteau plutons [*Irving et al.*,

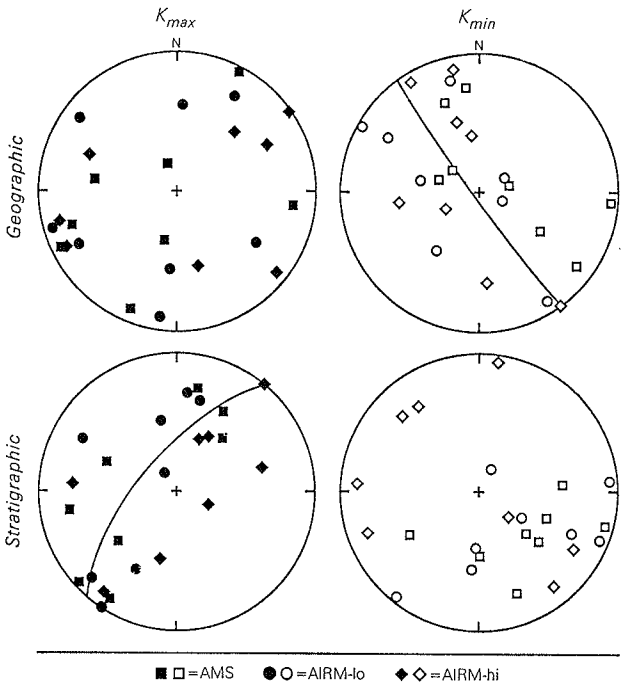

Figure 12. Inconclusive "fold test" on the anisotropy. The site-mean directions of maximum and minimum susceptibility (AMS, AIRM-lo, and AIRM-hi) are plotted in both geographic and stratigraphic coordinates. Weak planar trends for K_{max} in geographic coordinates and for K_{min} in statigraphic coordinates are indicated by best fit great circles. (Equal-area projection; lower hemisphere.)

Table 5. Effect of Anisotropy on Remanence Direction

		Remanence			Inferred Field			Effect	
Samples	N	D	I	k	D	I	k	dI	dS
				AMS					
HCS-1	9	325.8	70.1	47.7	336.4	69.9	55.2	0.2	+
HCS-2	8	352.2	63.0	18.5	356.5	65.0	20.8	-2.0	+
HCN-1	8	338.9	61.1	136.4	340.7	59.9	88.7	1.2	-
HCN-2	8	359.9	57.0	12.2	356.8	58.1	10.9	-1.1	-
HCN-3	7	356.3	57.3	32.6	355.7	62.1	29.2	-4.8	-
JH-1	5	343.1	38.0	83.8	339.1	37.6	87.3	0.4	+
JH-2	9	322.7	33.1	42.0	322.3	32.7	49.8	0.4	+
JH-3	7	352.5	58.3	101.4	355.0	61.3	118.0	-3.0	+
All	61	342.0	56.2	17.2	342.4	57.1	16.9	-0.9	-
				AIRM-lo					
HCS-1	3	301.4	70.8	96.2	308.9	69.6	53.2	1.2	-
HCS-2	3	7.9	60.0	8.4	16.8	64.5	9.1	-4.5	+
HCN-1	7	340.6	60.1	161.2	332.0	64.5	59.3	-4.4	-
HCN-2	4	354.3	62.7	27.9	357.0	60.7	15.4	2.0	-
HCN-3	4	2.4	54.3	36.3	2.3	61.6	31.1	-7.3	-
JH-1	2	334.4	36.8	--	328.4	34.7	--	2.1	?
JH-2	3	328.3	26.9	140.7	329.4	31.0	115.8	-4.1	-
JH-3	2	349.4	60.0	--	352.9	66.5	--	-6.5	?
All	28	343.4	56.8	17.8	343.4	59.6	16.7	-2.8	-
				AIRM-hi					
All	12	342.2	55.4	16.9	340.9	53.9	14.6	1.5	-

dI, difference between inclinations of remanence and inferred field (minus sign indicates that remanence is shallower than field); dS, change in dispersion caused by anisotropy (plus sign means that anistropy increased the dispersion so that remanence directions are more scattered than ancient field directions and minus sign means that anisotropy decreased the dispersion). Other symbols as in Table 1.

1985], and the Mount Stuart batholith [*Beck et al.*, 1981; *Ague and Brandon*, 1992]. Some [*Butler et al.*, 1989; *Brown and Burmester*, 1991] contended that this discordance is primarily explained by postmagnetization tilting of the individual plutons. This hypothesis was attractive in its economy: *Butler et al.* [1989] showed that only 29° of tilting about a properly oriented axis will produce the observed discordance. Some geobarometric data for the Spuzzum pluton [*Brown and Burmester*, 1991] lent support to this argument. The most straightforward evidence against the tilt hypothesis was the overall consistency of the remanence directions over the length of the southern part of the Coast Plutonic Complex and related rocks. Sites in plutonic rocks from Mount Stuart in the North Cascades of Washington to Stephens Island in the Coast Plutonic Complex just 100 km southeast of Duke Island (see Figure 1) all show northeasterly declinations and inclinations that are significantly shallow.

The mean paleomagnetic inclination for Duke Island, after making the compound structural correction, is 56° ± 10°, corresponding to a paleolatitude of 36° ± 10°. This result implies 3000 km (± 1300 km) of northward displacement relative to cratonal North America since the mid-Cretaceous (reference pole of *van Fossen and Kent* [1992]). *Irving et al.* [1985] inferred virtually the same amount of relative displacement from the remanence of intrusions in the Coast Plutonic Complex lacking indication of original horizontal.

The mean declination from Duke Island (344° ± 14°) is rotated 12° ± 17° clockwise with respect to the expected direction for North America, not formally significant, but significantly different from (and well short of) the clockwise rotations ranging from 36° to 67° implied by the results from the Coast Plutonic Complex cited above. This discordance implies the existence of a structural break between Duke Island and the Coast Plutonic Complex, along which more than 24° of differential rotation occurred but without significant relative latitudinal movements. *Saleeby* [1992] shows a set of thrust faults related to the mid-Cretaceous orogeny that lie just northeast of Duke Island. It is quite possible that at least part of the inferred rotation occurred along these structures.

Shown in the form of paleomagnetic poles in Figure 13, these paleomagnetic results may be compared to the mid-Cretaceous North American craton reference pole of *van Fossen and Kent* [1992], which covers the age range from 124 Ma to 88 Ma, the time of the well-known "Cretaceous stillstand". In Figure 13 we have included coeval poles from displaced terranes in the Inter-

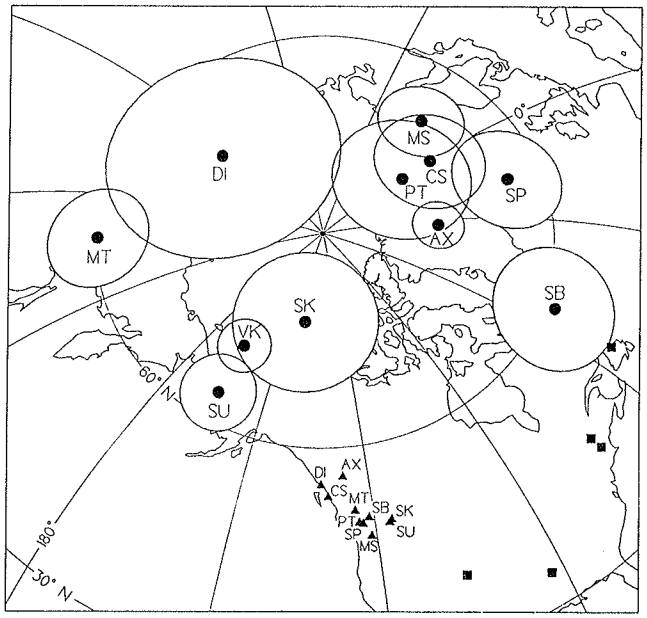

Figure 13. Equal-area map of part of northern hemisphere; projection is centered on Duke Island. Triangles are paleomagnetic sampling localities in the Canadian Cordillera, and filled circles are paleomagnetic poles encircled by 95% confidence limits. DI, Duke Island (this paper); MS, Mt. Stuart ([*Beck and Noson*, 1972; *Beck et al.*, 1981], incorporating the structural correction of *Ague and Brandon* [1992]); CS, Captain Cove and Stephens Island plutons [*Symons*, 1977]; PT, Porteau pluton [*Irving et al.*, 1995a]; SP, Spuzzum pluton [*Irving et al., 1985*]; MT, Mt. Tatlow volcanic and sedimentary rocks [*Wynne et al., 1995*]; AX, Axelgold layered gabbro, corrected for attitude of layering [*Monger and Irving*, 1980; *Armstrong et al.*, 1985]; SB, Spences Bridge Group [*Irving et al.*, 1995b]; SU, Summit Stock; SK, Skelly Creek Batholith [*Irving and Archibald*, 1990]; VK, mid-Cretaceous reference pole for North American craton [*van Fossen and Kent*, 1992]. Source data localities for VK are shown as squares.

montane superterrane as well as poles from intrusive rocks east of the displaced terranes. The locations of the rocks from which these poles were obtained are also shown in Figure 1. The Axelgold gabbro is a layered intrusion in the Cache Creek terrane on the east side of the Intermontane superterrane, from which some of the first discordant paleomagnetic results in the Canadian Cordillera were obtained [*Monger and Irving,* 1980]. It was subsequently more securely dated at 120-130 Ma [*Armstrong et al.,* 1985]. Although the choice is not clearcut, we show here the results after correction for the igneous layering (E. Irving, personal communication, 1993). An unequivocal southerly paleolatitude has recently been described by *Wynne et al.* [1995] from Late Cretaceous volcanic and sedimentary rocks in the Mount Tatlow area on the eastern flank of the Coast Plutonic Complex; this is the first such confirmatory result from bedded rocks within that superterrane. Another convincing mid-Cretaceous (104.5 ± 0.3 Ma) discordant paleolatitude has been obtained from bedded rocks of the Spences Bridge Group [*Irving et al.,* 1995b]; these rocks overlie all three terranes of the Intermontane superterrane [*Thorkelson and Smith,* 1989]. By way of contrast and confirmation we also show in Figure 13 two concordant paleomagnetic poles from coeval (94-100 Ma) plutonic rocks that intrude the Omineca Crystalline Belt to the east; the attitudes of these plutons have been evaluated using bathozonal mineral assemblages in their contact aureoles [*Irving and Archibald,* 1990].

Figure 14 shows the same paleomagnetic data as Figure 13 but recast as paleolatitudinal displacements of Cretaceous rocks. We have added the results from the Carmacks Group [*Marquis and Globerman,* 1988] as originally presented but referred to the 76 Ma cratonal pole from west-central Montana of *Gunderson and Sheriff* [1991]. The westward increase of Cretaceous paleolatitude anomaly across the superterranes has been previously noted by *Irving and Wynne* [1990]. The Coast Plutonic Complex and the Alexander terrane (and by implication Wrangellia, rocks of which are intruded by plutons of the Coast Plutonic Complex) have moved together latitudinally through about 25° northward since mid-Cretaceous time and have moved more than twice as far as rocks of the Intermontane superterrane. Concordant paleomagnetic results from widely distributed sites in rocks ranging in age from 48 Ma to 54 Ma show that these latitudinal movements were complete before middle Eocene time [*Irving and Brandon,* 1990; *Vandall and Palmer,* 1990; *Symons and Wellings,* 1989; *Bardoux and Irving,* 1989; *Fox and Beck,* 1985].

Debate on the mid-Cretaceous latitude of the Coast Plutonic Complex is still very lively. As Cowan [1994] has emphasized, geologic as well as paleomagnetic data will be crucial in moving the Baja BC issue toward resolution. Upward of 1000 km of right-lateral displacement can be reasonably inferred from offset geologic features on the Tintina-Rocky Mountain Trench and related faults that occur along the eastern edge of the Intermontane superterrane [*Gabrielse,* 1985]. *Umhoefer* [1987] has presented a plausible plate tectonic model for how northward displacement of the superterranes might have occurred. A quite different kind of evidence, fission track analysis of detrital zircons in arkosic sediments of the Methow-Pasayten basin at the southeast corner of the Coast Plutonic Complex, also supports a low paleolatitude of origin for these rocks [*Garver and Brandon,* 1994]. These authors conclude that although the provenance could have been the Omineca Crystalline Belt directly to the east of the present location of the basin, a preferable source may be

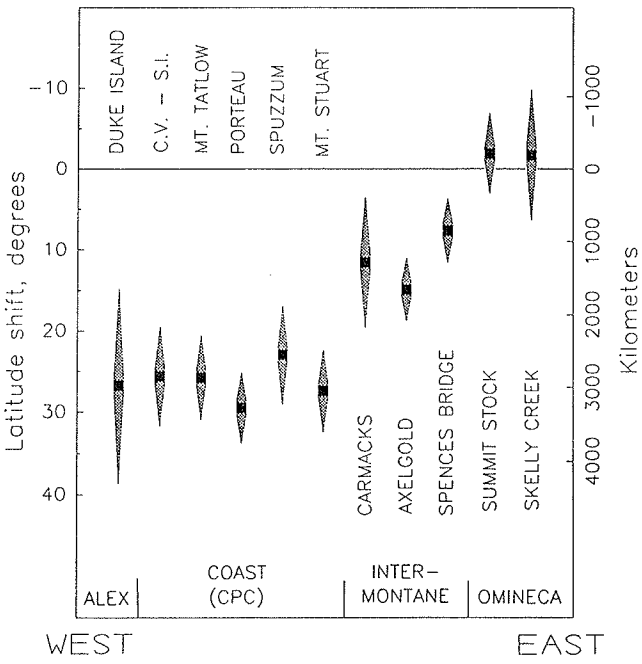

Figure 14. Paleolatitude difference diagram for Cretaceous rocks of the Canadian Cordillera and southeastern Alaska. Post-Cretaceous latitude shifts (positive northward) are the differences between the observed paleomagnetic paleolatitudes and those predicted from the appropriate reference pole for the North American craton. The shaded intervals are the 99% confidence limits about the latitude differences; the tapers represent schematically the diminishing probabilities of values farther from the means, and note as well that greater paleolatitude differences are equally as likely as lesser ones [*Irving and Wynne,* 1990]. All data are as in Figure 13, except that the Late Cretaceous Carmacks Group result as originally published by *Marquis and Globerman* [1988] is included. For this comparison we use the appropriate cratonal reference pole of *Gunderson and Sheriff* [1991]. ALEX, Alexander terrane, including the rest of the Insular superterrane; COAST, Coast Plutonic Complex; INTERMONTANE, Intermontane superterrane, including Stikinia, Cache Creek, and Quesnellia terranes; OMINECA, autochthonous part of the Omineca Crystalline Belt; C.V. - S.I., Captain Cove and Stephens Island (CS on Figure 13).

the Peninsular Ranges batholith, which was at the latitude of central Mexico when it formed in mid-Cretaceous time.

In this context the paleomagnetism of Duke Island takes on a special significance. As mentioned in the introduction, the ultramafic complex on Duke Island is the same age, intrudes the same rocks, and yields the same mid-Cretaceous paleolatitude as the Coast Plutonic Complex. The ultramafic complex, however, is layered, so that the paleohorizontal is known. Moreover, the layering and remanence at Duke Island have both been folded while the rocks were hot enough that only "widespread incipient crystal plastic deformation reflecting minor penetrative strain" is observed petrographically [*Saleeby,* 1992, p. 521]. Hence there is no question that the age of magnetization is close to the radiometric age. The ancient remanence of the Duke Island ultramafic

complex therefore joins the growing body of geophysical and geological evidence consistent with the Baja BC hypothesis.

Conclusions

1. The mid-Cretaceous (106-119 Ma) ultramafic (intrusive) complex on Duke Island carries a very stable magnetic remanence, carried by fine (single domain or pseudosingle domain) magnetite inclusions exsolved in clinopyroxene and perhaps other ferromagnesian silicate grains.
2. The remanence predates an episode of folding of the primary igneous lamination that occurred very early in the history of the intrusion, after the rocks had cooled to at least 540°C but while they were still hot enough for some of the petrographic evidence of deformation to have partly annealed.
3. The ultramafic rocks on Duke Island are magnetically anisotropic; this feature is seen both in measurement of initial magnetic susceptibility and of low-field isothermal remanent magnetization.
4. The anisotropy, though strong, is not consistent in orientation and has had no systematic effect on the primary remanence direction (including no increase in directional dispersion).
5. At one site, it is clear that the anisotropy arises at least partially from secondary magnetite produced by the serpentinization of olivine. Geologic relations show that this component of the anisotropy is postfolding, and so it cannot have affected the primary remanence direction.
6. The mean paleomagnetic inclination, after compound tectonic correction, indicates that in mid-Cretaceous time Duke Island and its part of the Alexander terrane were situated 3000 ± 1300 km farther south, with respect to cratonal North America, than since middle Eocene time. Geologic relations discussed in the introduction imply that this result also applies to the Coast Plutonic Complex and the terranes of the Insular superterrane intruded by its plutons (Wrangellia and the Alexander terrane). We emphasize that there is no indication in the paleomagnetic data of large-scale relative transcurrent movement between the Insular superterrane and the Coast Plutonic Complex.
7. The mid-Cretaceous paleolatitude from Duke Island accords very well with those interpreted by *Beck et al.* [1981], *Irving et al.* [1985, 1995b], and *Ague and Brandon* [1992] from coeval but unlayered plutonic units in the Coast Plutonic Complex as well as that recorded by Late Cretaceous stratified rocks [*Wynne et al.*, 1995]. Moreover, the subsequent northward movement implied by this low paleolatitude occurred at just the time interval predicted for the extremely rapid (up to 200 mm/yr) northward travel of the Kula plate [*Engebretson et al.*, 1985; *Umhoefer*, 1987; *Irving and Wynne*, 1991]. The amount (3000 km) is less than the ~4300 km predicted by *Engebretson et al.*'s [1985] reconstruction but greater than the 2500 km predicted by *Stock and Molnar* [1988], whose plate reconstruction does not assume fixed hotspots. These are plausibility arguments only because, as *Irving and Wynne* [1991] have recently emphasized, the displaced Cordilleran terranes cannot have been both tightly coupled to the Kula plate and adjacent to the North American craton during their northward travel.

Acknowledgments. We thank Henry C. Berg for enabling us to work on Duke Island and G.A. (Bud) Bodding for taking us there in his MYTIME. We also thank Occidental College students Kecia Harris and Kenji Shintaku who performed two key phases of the laboratory work. Helpful reviews were provided by Peter Haeussler, Jon Hagstrum, Jane Wynne, and Bill MacDonald, to whom we are grateful.

Appendix

Determination of Exsolution Temperature for Magnetite Inclusions

Two sets of nearly opaque inclusions are visible in the clinopyroxenes, one oriented roughly parallel to the crystallographic x direction of the host, and one roughly parallel to the crystallographic z direction (the "X" and "Z" inclusions, respectively). The interface between inclusion and host is a layer of closest-packed oxygen atoms [*Fleet et al.*, 1980], and it is reasonable to assume that the precise angle between inclusion and host is that which minimizes the total strain of both lattices. Moreover, because the two lattices expand differently when heated, the angle between host and inclusion will be a function of the temperature. The observed angle thus preserves information about the temperature at which the inclusion exsolved from the host.

Fleet et al. [1980] used this idea to determine the temperature of exsolution of magnetite inclusions (which the calculation assumed to be pure) from clinopyroxenes in the Renzy Lake (Quebec) ultramafic complex. Although the inclusions at Duke Island are not pure magnetite, the clinopyroxene hosts ($En_{44}Fs_8Wo_{48}$ [*Irvine*, 1974, Figure 25]) are nearly identical to those at Renzy Lake ($En_{45}Fs_6Wo_{49}$), and so it seemed possible to apply *Fleet et al.*'s [1980] calculations directly to the inclusions from Duke Island. Using a universal stage to orient horizontally the crystallographic x-z plane of each clinopyroxene grain, we measured the angle between the X and Z inclusions and the Z inclusions and the cleavages parallel to z in the clinopyroxene. Each angle is a function of the temperature of exsolution. Agreement between the temperatures derived from the two angles is evidence that *Fleet et al.*'s [1980] calculation is applicable. We made approximately 20 measurements of each angle from a total of five clinopyroxene grains (three from HCN-1 and one each from HCN-2 and HCN-3). The within-grain standard deviation of the angles was of order of a degree, most of which is likely observational error. The average X-Z interinclusion angle for the five grains was 102.5° ± 0.7°, which translates on Figure 8 of *Fleet et al.* [1980] to an exsolution temperature of 520°C (+50°C, -60°C). The average Z-z inclusion-to-axis angle was 9.1° ± 0.2°, translating to an exsolution temperature of 550°C (± 30°C). The grand mean is thus 535°C, while the center of the 50° of overlap between the two estimates is 545°C. We therefore take 540° ± 25°C as a reasonable estimate of the temperature at which the magnetite inclusions exsolved from the host silicate. As mentioned in the text, this temperature hardly differs from the values of peak dJ/dT listed in Table 1.

AMS Methods

AMS measurements were made using a fluxgate-spinner magnetometer fitted with coils that maintain a 50-μT field perpendicular to the axis of the fluxgate probe. This instrument senses differences in susceptibility (see *Noltimier* [1971] for theory of operation). We used a standard susceptibility bridge to determine the axial susceptibilities of the samples and then solved for the magnitudes and directions of the principal susceptibilities

using the data from the spinner magnetometer. The relatively large magnitudes of the susceptibilities and anisotropies produced a strong signal that was easily detectable, and measurements on the spinner magnetometer of the three principal susceptibility (K_{nn}) differences were generally self-consistent to within 10%. We have not directly translated these differences into angular errors at the sample level because they appear to be small relative to the between-sample variation within each site. After averaging at the site level, we observe good correspondence between the susceptibility fabrics and other structural features of the rocks. The agreement demonstrates that *Ellwood*'s [1978] estimates of precision (better than 15°) for sample K_{nn} directions are applicable. The AMS of two samples were remeasured on a low-field torque meter, and 12 samples were remeasured on a Sapphire Instruments alternating-field susceptibility meter. In both cases, most of the results agreed well with those obtained using the spinner magnetometer, especially for the samples having the lowest ratios of remanent to induced magnetization (see Table 1).

The AMS of a sample is represented by a 3 x 3 matrix **K**, a second-rank tensor. This tensor relates the induced magnetization M and applied field H, both written as 3 x 1 column vectors, by M = **K**H. In the general case, M and H will not be parallel; that is, the anisotropy has the effect of deflecting the direction of magnetization away from that of the applied field. We measured the AMS for five to ten samples per site and then estimated the site-mean AMS by finding the average of sample AMS tensors, each normalized by setting trace(**K**)=1 [e.g., *Ernst and Pearce,* 1989]. The eigenvectors of this matrix represent the directions of maximum, intermediate, and minimum site-mean susceptibility; the eigenvalues represent the corresponding relative susceptibilities (i.e., K_{max}, K_{int}, and K_{min}).

AIRM Methods

We used a 10-cm Helmholtz coil originally designed for AF demagnetization to produce IRMs in various orientations. The cylindrical rock samples were placed in a cubical sample holder which fits in a v groove aligned parallel to the axis of the coil. By this method, the sample axes could be aligned with the applied field to within a degree. For a particular IRM field level (say 10 mT), we followed these steps to determine the anisotropy tensor: (1) Partially demagnetize the sample in a tumbling AF apparatus using a peak field strength of twice the IRM field (20 mT in this example). (2) Measure the NRM that remains (NRM_{20}). (3) Apply a 10 mT direct field in the +X direction for several seconds and then measure the remanence. The vector difference between this remanence and NRM_{20} is the IRM component IRM_{10x+}. (4) Repeat steps 1 and 3 with the IRM applied in the -X direction. The vector quantity (IRM_{10x+}- IRM_{10x-})/2, which is like an average of the two components added, is IRM_{10x}. The first row of the IRM anisotropy tensor will consist of the X, Y, and Z components of IRM_{10x}. (5) Repeat steps 1, 3, and 4 using direct fields along the Y axis. The X, Y, and Z components of IRM_{10Y} constitute the second row of the anisotropy tensor. (6) Repeat step 5 for Z. The X, Y, and Z components of IRM_{10Z} constitute the third row of the anisotropy tensor.

Unlike a low-field induced magnetization, an IRM is only approximately proportional to field strength and so its anisotropy is less well represented by a tensor than is the AMS [*Coe,* 1966]. We checked the tensor approximation for one sample (9H443, from site HCS-1) by applying direct fields of 20 mT in 12 different orientations (at 30° intervals) perpendicular to the cylindrical (z) axis of the sample. After applying the field in one orientation and measuring the IRM produced parallel to the applied field, we AF demagnetized with a peak-field strength of 40 mT and then repeated the procedure in the next orientation. The IRMs produced in this way provided a direct measure of the anisotropy that could be compared to that predicted from the AIRM tensor we had determined previously. The anisotropy (maximum/minimum) in this plane was approximately 1.2, and the average discrepancy between the observed and expected IRM components was 2.7%. If this sample is representative, then the tensor approximation describes the anisotropy to within a few percent, a level of accuracy that is certainly adequate for assessing the paleomagnetic fidelity of the samples.

We determined AIRM tensors at 10 mT and 20 mT for 28 samples and for twelve of these also determined the AIRM at 30 mT and 40 mT. For comparison with the AMS, which is sensitive to fabrics in the lowest coercivity grains, we isolated the anisotropy characteristic of higher coercivity fractions by using differences between the IRM components added at two field strengths. A side benefit of restricting attention to narrow coercivity intervals is that errors due to the nonlinearity of IRM acquisition are reduced. To examine the anisotropy in the coercivity range 10 mT to 20 mT, for example, we calculated the vector difference IRM_{20X}- IRM_{10x}; its X, Y, and Z components constitute the first row of what we refer to as the AIRM-lo tensor. The other two rows were calculated in the same way. Components from the vector differences between 40 mT and 30 mT IRMs constitute the AIRM-hi tensor. These tensors were normalized and summed as described above for the AMS determinations to define the site-mean AIRM.

Error Estimates for Site-Mean Anisotropy

We have followed the lead of *Constable and Tauxe* [1990] in using a bootstrap technique to estimate the errors on the site-mean anisotropy data. This technique is appropriate for situations, such as often arise in paleomagnetism, where the number of samples N is small (less than 25). For a site where N=10, the procedure is as follows: (1) Construct a "pseudosample" set by drawing a random set of N from the N normalized sample tensors for the site. In the typical pseudosample set, several of the sample tensors will be represented more than once, and several will not be represented at all. (2) Calculate the pseudosample mean tensor by summing the N tensors that were drawn. (3) Find the three eigenvectors and eigenvalues (maximum, intermediate, and minimum) of the pseudosample mean tensor. (4) Repeat steps 1, 2, and 3 1000 times, the result being three lists of 1000 eigenvectors and three lists of 1000 eigenvalues. The essence of the bootstrap method is to take the variation of the means generated by this pseudosampling scheme as representative of the variation one would find by drawing sample means from the actual distribution.

The next step is to describe the dispersion of each set of eigenvectors, and here our analysis differs slightly from that of *Constable and Tauxe* [1990]. We follow the recommendation of *Fisher et al.* [1987] and use their "simple method" for analyzing axial data. This method requires only that the eigenvectors, all means themselves, follow an asymptotic bivariate normal distribution as would be expected from the Central Limit Theorem.

complex therefore joins the growing body of geophysical and geological evidence consistent with the Baja BC hypothesis.

Conclusions

1. The mid-Cretaceous (106-119 Ma) ultramafic (intrusive) complex on Duke Island carries a very stable magnetic remanence, carried by fine (single domain or pseudosingle domain) magnetite inclusions exsolved in clinopyroxene and perhaps other ferromagnesian silicate grains.
2. The remanence predates an episode of folding of the primary igneous lamination that occurred very early in the history of the intrusion, after the rocks had cooled to at least 540°C but while they were still hot enough for some of the petrographic evidence of deformation to have partly annealed.
3. The ultramafic rocks on Duke Island are magnetically anisotropic; this feature is seen both in measurement of initial magnetic susceptibility and of low-field isothermal remanent magnetization.
4. The anisotropy, though strong, is not consistent in orientation and has had no systematic effect on the primary remanence direction (including no increase in directional dispersion).
5. At one site, it is clear that the anisotropy arises at least partially from secondary magnetite produced by the serpentinization of olivine. Geologic relations show that this component of the anisotropy is postfolding, and so it cannot have affected the primary remanence direction.
6. The mean paleomagnetic inclination, after compound tectonic correction, indicates that in mid-Cretaceous time Duke Island and its part of the Alexander terrane were situated 3000 ± 1300 km farther south, with respect to cratonal North America, than since middle Eocene time. Geologic relations discussed in the introduction imply that this result also applies to the Coast Plutonic Complex and the terranes of the Insular superterrane intruded by its plutons (Wrangellia and the Alexander terrane). We emphasize that there is no indication in the paleomagnetic data of large-scale relative transcurrent movement between the Insular superterrane and the Coast Plutonic Complex.
7. The mid-Cretaceous paleolatitude from Duke Island accords very well with those interpreted by *Beck et al.* [1981], *Irving et al.* [1985, 1995b], and *Ague and Brandon* [1992] from coeval but unlayered plutonic units in the Coast Plutonic Complex as well as that recorded by Late Cretaceous stratified rocks [*Wynne et al.*, 1995]. Moreover, the subsequent northward movement implied by this low paleolatitude occurred at just the time interval predicted for the extremely rapid (up to 200 mm/yr) northward travel of the Kula plate [*Engebretson et al.*, 1985; *Umhoefer*, 1987; *Irving and Wynne*, 1991]. The amount (3000 km) is less than the ~4300 km predicted by *Engebretson et al.*'s [1985] reconstruction but greater than the 2500 km predicted by *Stock and Molnar* [1988], whose plate reconstruction does not assume fixed hotspots. These are plausibility arguments only because, as *Irving and Wynne* [1991] have recently emphasized, the displaced Cordilleran terranes cannot have been both tightly coupled to the Kula plate and adjacent to the North American craton during their northward travel.

Acknowledgments. We thank Henry C. Berg for enabling us to work on Duke Island and G.A. (Bud) Bodding for taking us there in his MYTIME. We also thank Occidental College students Kecia Harris and Kenji Shintaku who performed two key phases of the laboratory work. Helpful reviews were provided by Peter Haeussler, Jon Hagstrum, Jane Wynne, and Bill MacDonald, to whom we are grateful.

Appendix

Determination of Exsolution Temperature for Magnetite Inclusions

Two sets of nearly opaque inclusions are visible in the clinopyroxenes, one oriented roughly parallel to the crystallographic x direction of the host, and one roughly parallel to the crystallographic z direction (the "X" and "Z" inclusions, respectively). The interface between inclusion and host is a layer of closest-packed oxygen atoms [*Fleet et al.*, 1980], and it is reasonable to assume that the precise angle between inclusion and host is that which minimizes the total strain of both lattices. Moreover, because the two lattices expand differently when heated, the angle between host and inclusion will be a function of the temperature. The observed angle thus preserves information about the temperature at which the inclusion exsolved from the host.

Fleet et al. [1980] used this idea to determine the temperature of exsolution of magnetite inclusions (which the calculation assumed to be pure) from clinopyroxenes in the Renzy Lake (Quebec) ultramafic complex. Although the inclusions at Duke Island are not pure magnetite, the clinopyroxene hosts ($En_{44}Fs_8Wo_{48}$ [*Irvine*, 1974, Figure 25]) are nearly identical to those at Renzy Lake ($En_{45}Fs_6Wo_{49}$), and so it seemed possible to apply *Fleet et al.*'s [1980] calculations directly to the inclusions from Duke Island. Using a universal stage to orient horizontally the crystallographic x-z plane of each clinopyroxene grain, we measured the angle between the X and Z inclusions and the Z inclusions and the cleavages parallel to z in the clinopyroxene. Each angle is a function of the temperature of exsolution. Agreement between the temperatures derived from the two angles is evidence that *Fleet et al.*'s [1980] calculation is applicable. We made approximately 20 measurements of each angle from a total of five clinopyroxene grains (three from HCN-1 and one each from HCN-2 and HCN-3). The within-grain standard deviation of the angles was of order of a degree, most of which is likely observational error. The average X-Z interinclusion angle for the five grains was 102.5° ± 0.7°, which translates on Figure 8 of *Fleet et al.* [1980] to an exsolution temperature of 520°C (+50°C, -60°C). The average Z-z inclusion-to-axis angle was 9.1° ± 0.2°, translating to an exsolution temperature of 550°C (± 30°C). The grand mean is thus 535°C, while the center of the 50° of overlap between the two estimates is 545°C. We therefore take 540° ± 25°C as a reasonable estimate of the temperature at which the magnetite inclusions exsolved from the host silicate. As mentioned in the text, this temperature hardly differs from the values of peak dJ/dT listed in Table 1.

AMS Methods

AMS measurements were made using a fluxgate-spinner magnetometer fitted with coils that maintain a 50-μT field perpendicular to the axis of the fluxgate probe. This instrument senses differences in susceptibility (see *Noltimier* [1971] for theory of operation). We used a standard susceptibility bridge to determine the axial susceptibilities of the samples and then solved for the magnitudes and directions of the principal susceptibilities

According to *Fisher et al.* [1987], the simple method yields confidence cones very similar to those found via Bingham theory, which has more stringent requirements on the distribution and is computationally more complex. *Constable and Tauxe* [1990] assume that axial data follow a certain vectorial distribution (the "FB5" distribution of *Fisher et al.* [1987]). Although their approach yields very reasonable looking error limits, it seems conceptually neater to us to avoid treating axes as if they were vectors.

The simple method finds the mean axis (with 95% confidence limits) of a bipolar distribution or the pole (with confidence limits) to a girdle distribution, and in some cases it is a subjective choice which to report. Notice that the eigenvectors of the site-mean susceptibility tensor will usually differ by a few degrees from means derived (by whatever method) from the bootstrapped distributions. We use the former to characterize the site-mean AMS orientation and use the latter in defining the 95% confidence region (which therefore may not exactly center on site-mean directions). In addition, the site-mean eigenvectors are exactly orthogonal, whereas the axes derived from the bootstrapping are only close to orthogonal. Both kinds of data are listed in the Table 4.

For error limits on the normalized site-mean principal susceptibilities, we use "empirical" confidence limits [*Constable and Tauxe,* 1990]. The procedure here is to sort each list of 1000 eigenvalues generated by the bootstrap and then take the 50th and 950th elements as the lower and upper 95% confidence limits. As with the directional data, the values derived from the site-mean susceptibility tensor may not exactly center in the confidence limits derived from the bootstrapping.

References

Ague, J. J., and M. T. Brandon, Tilt and northward offset of Cordilleran batholiths resolved using igneous barometry, *Nature, 360*, 146-149, 1992.

Armstrong, R. L., J. W. H. Monger, and E. Irving, Age of magnetization of the Axelgold layered gabbro, north-central British Columbia, *Can. J. Earth Sci., 22*, 1217-1222, 1985.

Bardoux, M., and E. Irving, Paleomagnetism of Eocene rocks of the Kelowna and Castlegar areas: Studies in determining paleohorizontal, *Can. J. Earth Sci., 26*, 829-844, 1989.

Beck, M. E., Jr., and L. Noson, Anomalous paleolatitudes in Cretaceous granitic rocks, *Nature, 235*, 11-13, 1972.

Beck, M. E., Jr., R. F. Burmester, and R. Schoonover, Paleomagnetism and tectonics of the Cretaceous Mt. Stuart batholith of Washington: Translation or tilt?, *Earth Planet. Sci. Lett., 56*, 336-342, 1981.

Brown, E. H., and R. F. Burmester, Metamorphic evidence for the tilt of the Spuzzum Pluton: Diminished basis for the "Baja British Columbia" concept, *Tectonics, 10*, 978-985, 1991.

Butler, R. F., G. E. Gehrels, W. C. McClelland, S. R. May, and D. Klepacki, Discordant paleomagnetic poles from the Canadian Coast Plutonic Complex: Regional tilt rather than large-scale displacement?, *Geology, 17*, 691-694, 1989.

Butler, R. F., W. R. Dickinson, G. E. Gehrels, W. C. McClelland, S. R. May, and D. Klepacki, Reply to comment on "Discordant paleomagnetic poles from the Canadian Coast Plutonic Complex: Regional tilt rather than large scale displacement?, *Geology, 18*, 1165-1166, 1990a.

Butler, R. F., G. E. Gehrels, W. C. McClelland, S. R. May, and D. Klepacki, Reply to comment on "Discordant paleomagnetic poles from the Canadian Coast Plutonic Complex: Regional tilt rather than large-scale displacement?", *Geology, 18*, 801-802, 1990b.

Coe, R. S., Analysis of magnetic shape anisotropy using second-rank tensors, *J. Geophys. Res., 71*, 2637-2644, 1966.

Constable, C., and L. Tauxe, The bootstrap for magnetic susceptibility tensors, *J. Geophys. Res., 95*, 8383-8395, 1990.

Cowan, D. S, Alternative hypotheses for the mid-Cretaceous paleogeography of the western Cordillera, *GSA Today, 4*, 181-186, 1994.

Davis, K. E., Magnetite rods in plagioclase as the primary carrier of stable NRM in ocean floor gabbros, *Earth Planet. Sci. Lett., 55*, 190-198, 1981.

Ellwood, B. B., Measurement of anisotropy of magnetic susceptibility: A comparison of the precision of torque and spinner magnetometer systems for basaltic specimens, *J. Phys. E Sci. Instrum., 11*, 71-75, 1978.

Engebretson, D. C., A. Cox, and R. Gordon, Relative motions between oceanic and continental plates in the Pacific basin, *Spec. Pap. Geol. Soc. Am., 206*, 1-59, 1985.

Ernst, R. E., and G. W. Pearce, Averaging of anisotropy of magnetic susceptibility data, in *Statistical Applications in the Earth Sciences*, edited by F. P. Agterberg and G. F. Bonham-Carter, pp. 297-305, Geol. Surv. of Can., Ottawa, 1989.

Evans, M. E., M. W. McElhinny, and A. C. Gifford, Single domain magnetite and high coercivities in a gabbroic intrusion, *Earth Planet. Sci. Lett., 4*, 142-146, 1968.

Fisher, N. I., T. Lewis, and B. J. J. Embleton, *Statistical Analysis of Spherical Data*, Cambridge Univ. Press, New York, 1987.

Fleet, M. E., G. A. Bilcox, and R. L. Barnett, Oriented magnetite inclusions in pyroxenes from the Grenville province, *Can. Mineral., 18*, 89-99, 1980.

Fox, K. F., and M. E. Beck, Jr., Paleomagnetic results for Eocene volcanic rocks from northeastern Washington and the Tertiary tectonics of the Pacific Northwest, *Tectonics, 3*, 323-341, 1985.

Gabrielse, H., Major dextral transcurrent displacements along the Northern Rocky Mountain Trench and related lineaments in north-central British Columbia, *Geol. Soc. Am. Bull., 96*, 1-14, 1985.

Garver, J. I., and M. T. Brandon, Fission-track ages of detrital zircons from Cretaceous strata, southern British Columbia: Implications for the Baja BC hypothesis, *Tectonics, 13*, 401-420, 1994.

Gehrels, G. E., and H. C. Berg, Geologic map of southeastern Alaska, *U. S. Geol. Surv. Open File Rep., 84-886*, 28 pp., 1984.

Gehrels, G. E., J. B. Saleeby, and H. C. Berg, Geology of Annette, Gravina, and Duke Islands, southeastern Alaska, *Can. J. Earth Sci., 24*, 866-881, 1987.

Gehrels, G. E., W. C. McClelland, S. D. Samson, P. J. Patchett, and J. L. Jackson, Ancient continental margin assemblage in the northern Coast Mountains, southeast Alaska and northwest Canada, *Geology, 18*, 208-211, 1990.

Gunderson, J. A., and S. D. Sheriff, A new Late Cretaceous paleomagnetic pole from the Adel Mountains, west central Montana, *J. Geophys. Res., 96*, 317-326, 1991.

Haeussler, P., Structural evolution of an arc-basin: The Gravina Belt in central southeastern Alaska, *Tectonics, 11*, 1245-1265, 1992.

Hargraves, R. B., Magnetic anisotropy and remanent magnetism in hemo-ilmenite from ore deposits at Allard Lake, Quebec, *J. Geophys. Res., 64*, 1565-1578, 1959.

Hargraves, R. B., and W. M. Young, Source of the stable remanent magnetization of the Lambertville diabase, *Am. J. Sci., 267*, 1161-1177, 1969.

Irvine, T. N., Petrology of the Duke Island ultramafic complex, southeastern Alaska, *Mem. Geol. Soc. Am., 138*, 1-240, 1974.

Irving, E., and D. A. Archibald, Bathozonal tilt corrections to paleomagnetic data from the mid-Cretaceous plutonic rocks: Examples from the Omineca Crystalline Belt, British Columbia, *J. Geophys. Res., 95*, 4579-4585, 1990.

Irving, E., and M. T. Brandon, Paleomagnetism of the Flores volcanics, Vancouver Island, in place by Eocene time, *Can. J. Earth Sci., 27*, 811-817, 1990.

Irving, E., and P. J. Wynne, Paleomagnetic evidence bearing on the evolution of the Canadian Cordillera, *Philos. Trans. R. Soc. London A, 331*, 487-509, 1990.

Irving, E., and P. J. Wynne, Paleomagnetic evidence for motions of parts of the Canadian Cordillera, *Tectonophys., 187*, 259-275, 1991.

Irving, E., G. J. Woodsworth, P. J. Wynne, and A. Morrison, Paleomagnetic evidence for displacement from the south of the Coast Plutonic Complex, British Columbia, *Can. J. Earth Sci., 22*, 584-598, 1985.

Irving, E., J. Baker, N. Wright, C. J. Yorath, R. J. Enkin, and D. York, Magnetism and age of the Porteau Pluton, southern Coast Plutonic Complex, British Columbia: Evidence for tilt and translation, *Can. J. Earth Sci.*, in the press, 1995a.

Irving, E., D. J. Thorkelson, P. M. Wheadon, and R. J. Enkin, Paleomagnetism of the Spences Bridge Group and northward displacement of the Intermontane Belt, British Columbia: a second look, *J. Geophys. Res., 100*, 6057-6071, 1995b.

Lanphere, M. A., and G. D. Eberlein, Potassium-argon ages of magnetite-bearing ultramafic complexes in southeastern Alaska, *Spec. Pap. Geol. Soc. Am., 87*, 94, 1966.

MacDonald, W. D., and B. B. Ellwood, Magnetic fabric of peridotite with intersecting

petrofabric surfaces, Tinaquillo, Venezuela, *Phys. Earth Planet. Inter.*, *51*, 301-312, 1988.

Marquis, G., and B. R. Globerman, Northward motion of the Whitehorse Trough: Paleomagnetic evidence from the Upper Cretaceous Carmacks Group, *Can. J. Earth Sci.*, *25*, 2005-2016, 1988.

McClelland, W. C., G. E. Gehrels, S. D. Samson, and P. J. Patchett, Structural and geochronologic relations along the western flank of the Coast Mountains batholith: Stikine River to Cape Fanshaw, central southeastern Alaska, *J. Struct. Geol.*, *14*, 475-489, 1992.

McFadden, P. L., and D. L. Jones, The fold test in palaeomagnetism, *Geophys. J. R. Astron. Soc.*, *67*, 53-58, 1981.

Meen, J. K., L. W. Snee, K. Ross, and D. Elthon, Age and geologic relationships of the Hall Cove Complex, Duke Island, southeastern Alaska, *Geol. Soc. Am. Abstr. Programs.*, *23*, A389, 1991.

Miller, R. B., S. Y. Johnson, and J. W. McDougall, Comment on "Discordant paleomagnetic poles from the Canadian Coast Plutonic Complex: Regional tilt rather than large-scale displacement?", *Geology*, *18*, 1164-1165, 1990.

Monger, J. W. H., and E. Irving, Northward displacement of north-central British Columbia, *Nature*, *285*, 289-294, 1980.

Monger, J. W. H., R. A. Price, and D. J. Tempelman-Kluit, Tectonic accretion and the origin of the two major metamorphic and plutonic welts in the Canadian Cordillera, *Geology*, *10*, 70-75, 1982.

Murthy, G. S., M. E. Evans, and D. I. Gough, Evidence of single domain magnetite in the Michikamau anorthosite, *Can. J. Earth Sci.*, *8*, 361-370, 1971.

Nokleberg, W. J., et al., Circum-north Pacific tectonostratigraphic terrane map, *U. S. Geol. Surv. Open File Rep.*, *94-714*, 221 pp., 1994.

Noltimier, H. C., Determining magnetic anisotropy of rocks with a spinner magnetometer giving in-phase and quadrature output, *J. Geophys. Res.*, *76*, 4849-4854, 1971.

Rubin, C. M., and J. B. Saleeby, Tectonic history of the eastern edge of the Alexander Terrane, southeast Alaska, *Tectonics*, *11*, 586-602, 1992.

Rubin, C. M., J. B. Saleeby, D. S. Cowan, M. T. Brandon, and M. F. McGroder, Regionally extensive mid-Cretaceous west-vergent thrust system in the northwestern Cordillera: Implications for continent-margin tectonism, *Geology*, *18*, 276-280, 1990.

Rusmore, M. E., and G. J. Woodsworth, Coast Plutonic Complex: A mid-Cretaceous contractional orogen, *Geology*, *19*, 941-944, 1991.

Saleeby, J. B., Age and tectonic setting of the Duke Island ultramafic intrusion, southeast Alaska, *Can. J. Earth Sci.*, *29*, 506-522, 1992.

Silberling, N. J., and D. L. Jones, Lithotectonic terrane maps of the North American Cordillera, *U. S. Geol. Surv. Open File Rep.*, *84-523*, B1-B31, 1984.

Smith, J. G., and M. F. Diggles, Potassium-argon determinations in the Ketchikan and Prince Rupert quadrangles, southeastern Alaska, *U. S. Geol. Surv. Open File Rep.*, *78-73N*, 1981.

Stephenson, A., S. Sadikun, and D. K. Potter, A theoretical and experimental comparison of the anisotropies of magnetic susceptibility and remanence in rocks and minerals, *Geophys. J. R. Astron. Soc.*, *84*, 185-200, 1986.

Stock, J., and P. Molnar, Uncertainties and implications of the Late Cretaceous and Tertiary positions of North America relative to the Farallon, Kula, and Pacific plates, *Tectonics*, *7*, 1339-1384, 1988.

Symons, D. T. A., Paleomagnetism of Mesozoic plutons in the westernmost Coast Complex of British Columbia, *Can. J. Earth Sci.*, *14*, 2127-2139, 1977.

Symons, D. T. A., and M. R. Wellings, Paleomagnetism of the Eocene Kamloops Group and the cratonization of Terrane I of the Canadian Cordillera, *Can. J. Earth Sci.*, *26*, 821-828, 1989.

Taylor, H. P., The zoned ultramafic complexes of southeastern Alaska, in *Ultramafic and Related Rocks*, edited by P. J. Wyllie, pp. 96-118, John Wiley, New York, 1967.

Thorkelson, D. J., and A. D. Smith, Arc and intraplate volcanism in the Spences Bridge Group: Implications for Cretaceous tectonics in the Canadian Cordillera, *Geology*, *17*, 1093-1096, 1989.

Tipper, H. W., G. J. Woodsworth, and H. Gabrielse, Tectonic assemblage map of the Canadian cordillera and adjacent parts of the United States of America, *Map 1505A*, Geol. Surv. of Can., Ottawa, Ont., 1981.

Umhoefer, P. J., Northward translation of "Baja British Columbia" along the Late Cretaceous to Paleocene margin of western North America, *Tectonics*, *6*, 377-394, 1987.

Umhoefer, P. J., and J. E. Magloughlin, Comment on "Discordant paleomagnetic poles from the Canadian Coast Plutonic Complex: Regional tilt rather than large-scale displacement?", *Geology*, *18*, 800-801, 1990.

Vandall, T. A., and H. C. Palmer, Upper limit of docking time for Stikinia and Terrane I: Paleomagnetic evidence from the Eocene Ootska Lake Group, British Columbia, *Can. J. Earth Sci.*, *27*, 212-218, 1990.

Van der Heyden, P., A Middle Jurassic to Early Tertiary Andean-Sierran arc model for the Coast Belt of British Columbia, *Tectonics*, *11*, 82-97, 1992.

van Fossen, M. C., and D. V. Kent, Paleomagnetism of 122 Ma plutons in New England and the mid-Cretaceous paleomagnetic field in North America: True polar wander or large-scale differential mantle motion?, *J. Geophys. Res.*, *97*, 19651-19661, 1992.

Wynne, P. J., E. Irving, J. A. Maxson, and K. L. Kleinspehn, Paleomagnetism of the Upper Cretaceous strata of Mt. Tatlow: Evidence for 3000 km of northward displacement of the eastern Coast Belt, British Columbia, *J. Geophys. Res.*, *100*, 6073-6091, 1995.

S. W. Bogue, Department of Geology, Occidental College, 1600 Campus Road, Los Angeles, CA 90041. (e-mail: bogue@oxy.edu)

S. Gromme, and J. Hillhouse, U.S. Geological Survey, 345 Middlefield Road, Menlo Park, CA 94025. (e-mail: csgromme@mojave.wr.usgs.gov; jhillhouse@isdmnl.wr.usgs.gov)

(Received June 24, 1994;
revised April 25, 1995;
accepted May 24, 1995.)